NASA Technical Memorandum 112213

Moving-Base Simulation Evaluation of Control/Display Integration Issues for ASTOVL Aircraft

James A. Franklin, Ames Research Center, Moffett Field, California

November 1997

National Aeronautics and
Space Administration

Ames Research Center
Moffett Field, California 94035-1000

Moving-Base Simulation Evaluation of Control/Display Integration Issues for ASTOVL Aircraft

JAMES A. FRANKLIN

Ames Research Center

Summary

A moving-base simulation has been conducted on the Vertical Motion Simulator at Ames Research Center using a model of an advanced, short takeoff and vertical landing (STOVL) lift fan fighter aircraft. This experiment expanded on investigations during previous simulations with this STOVL configuration with the objective of evaluating (1) control law modifications over the low speed flight envelope, (2) integration of the throttle inceptor with flight control laws that provide direct thrust command for conventional flight, vertical and short takeoff, and flightpath or vertical velocity command for transition, hover, and vertical landing, (3) control mode blending for pitch, roll, yaw, and flightpath control during transition from wing-borne to jet-borne flight, and (4) effects of conformal versus nonconformal presentation of flightpath and pursuit guidance symbology on the out-the-window display for low speed STOVL operations. Assessments were made for takeoff, transition, hover, and landing, including precision hover and landing aboard an LPH-type amphibious assault ship in the presence of winds and rough seas.

Results yielded Level 1 pilot ratings for the flightpath and vertical velocity command modes for a range of land-based and shipboard operation and were consistent with previous experience with earlier control laws and displays for this STOVL concept. Control mode blending was performed over speed ranges in accord with the pilot's tasks and with the change of the basic aircraft's characteristics between wing-borne and hover flight. Blending of yaw control from heading command in hover to sideslip command in wing-borne flight performed over a broad speed range helped reduce yaw transients during acceleration through the low speed regime. Although the pilots appreciated conformality of flightpath and guidance symbols with the external scene during the approach, increased sensitivity of the symbols for lateral path tracking elevated the pilots' control activity in the presence of turbulence. The pilots preferred the choice of scaling that was originally established during the display development and in-flight evaluations.

Introduction

Ames Research Center has participated in the definition and evaluation of integrated flight/propulsion control concepts and design guidelines in support of development of short takeoff and vertical landing (STOVL) configurations for the Joint Strike Fighter program. Contributions have come from the flight research program on NASA's vertical or short takeoff and landing (V/STOL) Systems Research Aircraft (VSRA) described in reference 1 and from experiments on the Vertical Motion Simulator with different STOVL designs (refs. 2–4). These flight and simulation experiments have addressed issues of control and display modes for different phases of STOVL operations—control power, thrust margin, transition acceleration, and control system dynamic response requirements. Over the past few years, two moving-base simulations of a lift-fan configuration were used in the design guideline development (refs. 5 and 6).

Based on the results of those flight and simulation programs, modifications were made to the control system, head-up display (HUD), and propulsion system of the lift fan configuration to improve the integrated flight/propulsion control and display system concept and to address integration issues that were not fully investigated in references 5 and 6. In particular, the control system was altered to incorporate nonlinear inverse control laws in all axes. In the earlier simulations, the nonlinear inverse appeared in the augmented control on longitudinal and vertical velocity and for yaw control in forward flight. The inverse scheme is now employed in all axes of control. State rate feedback control has been eliminated in the control system, with the exception of the vertical axis, based on concerns of the practical utility of angular accelerometers for pitch, roll, and yaw control, and of the need to use linear accelerometers to achieve acceptable control response and disturbance suppression for control of longitudinal and lateral velocity in hover.

For the control modes implemented in this control concept, the throttle serves alternately as an inceptor for thrust and for vertical velocity control depending on control mode selected. The ability to scale the inceptor commands to the propulsion system so as to be free of

transients at mode switch and to provide satisfactory control sensitivity and full control authority to the pilot is a major design concern. New schemes for scaling the throttle inceptor for use as a thrust or vertical velocity controller for approach and hover control in translational rate command mode, described in reference 7, were added to the model for assessment in this simulation.

Control mode blending continues to be difficult to resolve because of the conflicting demands of wing-borne and jet-borne tasks. The issues of importance are (1) the transition between pitch and roll attitude control modes appropriate for conventional and vertical flight, (2) the use of attitude to control flightpath in wing-borne and semi-jet-borne flight changing to thrust control of vertical velocity in vertical flight, (3) the control of yaw for low speed maneuvers and turn coordination to minimize sideslip in semi-jet-borne flight. Given concerns raised in the simulation of reference 6 of abrupt yaw transients associated with control law blending during acceleration to wing-borne flight, alternative control mode blending ranges were evaluated in this simulation to examine the effect on sideslip control during accelerating flight for takeoff and waveoff from low speed.

Advancing developments in helmet mounted displays (HMD) remove restrictions on display content imposed by the fixed optics of current head-up displays and permit consideration of symbology that registers against the external scene. In the past, narrow field-of-view HUD optics have made it necessary to scale commands to guidance and control elements to keep them within view in crosswinds and at low speed. While angular path relationships diminish in importance at low speed as the aircraft approaches the hover, they are appropriate at higher speeds in the approach to the landing pad. Of particular interest in this simulation was the presentation of lateral guidance and control information. Although HMD optics were not available, the HUD symbology was projected on the forward visual scene which had sufficient field of view to display the flightpath and ghost aircraft conformally down to low speeds where it is appropriate to shift the presentation to scaled vertical and lateral velocities. Thus, conformal as opposed to scaled presentation of the lateral displacement of the flightpath and ghost aircraft symbols were assessed to determine the merits of each.

The remainder of this report presents a brief description of the aircraft, a synopsis of the simulation experiment, and discussion of the results therefrom.

Nomenclature

K_ε	flightpath and ghost aircraft symbol scaling
N_β	directional stability, rad/sec^2/rad
S	wing area, ft^2
W	aircraft weight, lb

Acronyms

APP	approach control mode
ASTOVL	advanced short takeoff and vertical landing
CGI	computer-generated image
CTO	cruise/takeoff control mode
HMD	helmet mounted display
HQR	Cooper-Harper handling qualities rating
HUD	head-up display
IMC	instrument meteorological conditions
MTV	manual thrust vector control mode
rms	root mean square
SCAS	stability and command augmentation system
STOL	short takeoff and landing
STOVL	short takeoff and vertical landing
TRC	translational rate command control mode
VMC	visual meteorological conditions
VSRA	V/STOL Systems Research Aircraft
V/STOL	vertical or short takeoff and landing

Basic Lift Fan STOVL Aircraft

The lift fan STOVL aircraft is a single-place, single-engine, fighter/attack aircraft, featuring a wing-canard arrangement with twin vertical tails (fig. 1). The propulsion system concept is presented in figure 2. It consists of a remote lift fan coupled to a lift-cruise turbofan engine to permit continuous transfer of energy from the lift-cruise engine to the lift fan. Further, the lift-cruise engine exhaust is either ducted aft to a thrust-deflecting cruise nozzle in conventional flight or diverted to two deflecting lift nozzles in vertical flight. Throughout transition, flow can be continuously transferred between the cruise and lift nozzles. Lift fan and lift nozzle thrust can be deflected

downward from 45 to 100 deg relative to the aircraft waterline and lift nozzle thrust can be deflected 10 deg laterally as well. The cruise nozzle can be deflected ±20 deg relative to the aircraft waterline in the vertical plane. A full description of the simulation model is presented in references 7 and 8.

The basic flight control system consists of the canard, ailerons and twin rudders for aerodynamic effectors during forward flight. For powered-lift operation, control is provided by differential thrust transfer between the lift fan and lift nozzles, deflection of lift fan and lift nozzle thrust, and deflection of cruise nozzle thrust. Pitch control is achieved by a combination of canard deflection, thrust transfer between the lift fan and lift nozzles, and deflection of the cruise nozzle. Roll control is produced by the ailerons and differential thrust transfer between the lift nozzles. Yaw control is derived from the combination of rudder deflection and lateral deflection of lift nozzle thrust. As an option, reaction control, powered by engine compressor bleed air, can provide additional control moments through nozzles located in the wing extremities and in the tail. Longitudinal acceleration is achieved through thrust transfer between the lift fan, lift nozzles, and cruise nozzles and by deflection of the lift fan and lift nozzle thrust.

Four control modes are provided. They enable operation in all regimes of conventional wing-borne flight and jet-borne operation with manual thrust management consistent with current Harrier operations. In addition, they include control augmentation that provides for precise, low-workload control of the aircraft in jet-borne flight that permits operations in adverse weather conditions that are not achievable with the current Harrier fleet. The modes are summarized in table 1 and described in further detail in reference 7.

In the cruise/takeoff (CTO) mode, the aircraft can be flown conventionally for wing-borne takeoff, cruise, and landing. The pilot has direct control of lift-cruise engine thrust; however, the propulsive lift system is not in use, and the pilot has no direct control of thrust vector angle. Rate damping augmentation and angle-of-attack stability are provided for pitch control, rate command is provided for roll control, and sideslip command is included for yaw control. The manual thrust vector (MTV) mode provides for operation in jet-borne flight including vertical and short takeoff, transition, hover, and vertical and slow landing. In this mode, the pilot has manual control of the magnitude of the propulsion system thrust (lift fan plus lift-cruise engine thrust) and the deflection of the resultant thrust vector, thus allowing the aircraft to be configured and controlled for the phases of operation noted above.

No feedback control loops are used for either speed or flightpath control. Pitch and roll are controlled through rate command/attitude hold augmentation in transition, blending to attitude command/attitude hold at low speed.

Table 1. Flight control modes

Control axis	Control mode designations (applicable flight phases)			
	CTO (wing-borne flight)	MTV (transition, hover) APP (transition)	APP (transition, hover)	TRC (hover)
Pitch/roll	Rate command	Rate command – attitude hold, blend to attitude command	Rate command – attitude hold, blend to attitude command	
Yaw	Sideslip command	Sideslip command, blend to yaw rate command	Sideslip command, blend to yaw rate command	Yaw rate command
Vertical	Aerodynamic lift	Thrust magnitude	Flightpath command, blend to velocity command	Velocity command
Longitudinal	Thrust magnitude	Thrust vector angle (MTV), acceleration command – velocity hold (APP)	Acceleration command – velocity hold	Velocity command
Lateral				Velocity command

Yaw control is the same as for CTO at higher airspeeds during transition, and then blends to yaw rate command at low speed. The approach (APP) mode is designed to reduce workload and improve precision of control of the longitudinal and vertical response during the decelerating transition to hover or for slow landings. It provides the pilot with independent control of the longitudinal and vertical axes. In so doing, it activates a longitudinal acceleration command/velocity hold system, with thrust vector angle as the speed control effector. As the aircraft decelerates from wing-borne to jet-borne flight, a flightpath command augmentation system is activated when the propulsion system is configured to provide effective control of the vertical axis. This mode is engaged when the resultant thrust vector angle exceeds 70 deg and the commanded core engine thrust exceeds 60 percent of its maximum value. This system remains engaged until the net thrust vector angle decreases below 47 deg or the throttle angle is reduced below 20 percent of full throw. Until the flightpath command augmentation is engaged, the pilot still has direct control of lift-cruise engine thrust. When the throttle is advanced beyond 95 percent of full throw, direct command of thrust is once again available. The flightpath command system will then reengage once the throttle is reduced below 90 percent of full throw. Pitch, roll, and yaw control are identical to that for MTV. The translational rate command (TRC) mode is available for precision control of hover positioning and vertical landing. In this mode, decoupled command of longitudinal, lateral, and vertical velocity is provided. Longitudinal velocity control is achieved through deflection of the thrust vector at constant pitch attitude. Lateral velocity command is realized through roll control. The yaw axis control remains the same as that for MTV.

A HUD, described in detail in references 7, 9, and 10, provides the primary flight display for all phases of operation. A baseline set of symbology is presented for all flight regimes and is augmented by command and situation information for precision approach and hover. The baseline display included aircraft attitude, speed, flightpath angle, angle-of-attack reference, altitude, engine revolutions per minute, thrust vector angle, flap angle, longitudinal acceleration, heading, and distance to the hover point, as shown in figure 3. Symbology added to the display for precision-guided approach to hover are shown as well in figure 3. This information appears upon guidance selection in either the MTV or APP mode. The guidance display is a flightpath centered, pursuit presentation that enhances the external visual cues, centers them on the aircraft's flightpath, and presents the pilot with a pursuit tracking task for following the intended transition and approach guidance to a final hover point. Course and glideslope guidance are provided in the form of a leader (ghost) aircraft that follows the desired flight profile. The pilot's task is to track the ghost aircraft with the flightpath symbol. For the APP mode, deceleration guidance is presented by an acceleration error ribbon on the left side of the flightpath symbol which the pilot nulls to follow the deceleration schedule. When guidance is not selected, the guidance related symbols (ghost aircraft, acceleration error ribbon, longitudinal acceleration scale, landing deck, and glideslope reference line) are removed from the display. During the latter stages of the deceleration as the aircraft approaches the intended point of hover, selective changes are made to the approach display to provide guidance for the hover point capture. Specifically, the longitudinal velocity vector, predicted longitudinal velocity, and station-keeping cross appear referenced to the vertical velocity diamond symbol in plan view as shown in figure 4. The pilot controls the velocity predictor toward the station-keeping cross position and adjusts velocity to bring the cross to rest at the reference hover point indicated by the cross being adjacent to the vertical velocity diamond. When the TRC mode is selected for precision hover and vertical landing, the HUD format superimposes vertical and plan views and provides command and situation information in a pursuit tracking presentation (fig. 5). In the horizontal situation, the aircraft velocity vector is represented by a line emanating from the aircraft symbol. A pad symbol represents the landing area. Horizontal and vertical velocity predictor symbols, whose displacement and orientation from the aircraft symbol indicate magnitude and direction, provide the pilot lead information for hover maneuvering. Horizontal velocities commanded by the pilot through the control system are displayed directly by the predictor ball. The vertical situation is displayed by a diamond referenced to the right leg of the aircraft symbol. The diamond symbol is displayed against a vertical bar whose length represents the operational vertical velocity limits for the landing gear. The length of the bar is based on the vertical velocity relative to the landing pad. For shipboard operation, when vertical deck motion can be uplinked to the aircraft, the limit, as affected by relative closure rate to the deck, is presented on this symbol. This bar provides the pilot with an indication of sink rate margin for the vertical landing. A horizontal bar indicates the altitude remaining to touchdown. A panel-mounted head-down display presents a compass rose and a plan view of the reference flightpath following guidance select.

Inceptors available in the cockpit and their relation to response types for the various control modes are shown in figure 6. Individual inceptors are the center stick and trim switch, pedals, throttle lever, nozzle lever, throttle thumbwheel, and flap switch. The center stick commands pitch

and roll rate in CTO, pitch and roll rate command/attitude hold in MTV and APP at higher speeds, blending to attitude command/attitude hold at lower speeds, and longitudinal and lateral inertial velocity in TRC. The trim switch on the stick provides pitch and roll rate trim in CTO, and in MTV and APP in conjunction with the rate command/attitude hold response type. At low speed when the attitude command response type is functional, the trim switch provides attitude trim. In TRC, the trim switch adjusts the reference longitudinal and lateral inertial velocities. In CTO, pedals function as sideslip command, while in MTV and APP they provide sideslip command at high speed, blending to yaw rate command at low speed. The throttle controller commands total thrust magnitude in CTO and MTV modes, and in APP mode when flightpath command augmentation is not engaged. When flightpath command is engaged in APP mode, the throttle commands flightpath angle when ground speed is greater than 60 knots and vertical velocity when speed is less than 60 knots. In TRC, the throttle controls vertical velocity. The nozzle lever has the sole function of command of the resultant thrust vector angle in MTV. Otherwise, it is backdriven to a position consistent with the thrust vector angle being commanded for CTO, APP, or TRC modes, so as to be in the correct position when a switch occurs from any of these modes to MTV. Activation of the wave-off switch on the top of the nozzle lever will initiate a switch from any of these modes to MTV so long as the nozzle lever is in a position consistent with the current thrust vector angle. The throttle thumbwheel serves the function of command of longitudinal acceleration/velocity hold in APP mode. It is a proportional control with center detent and adjustable friction. When in the detent, the thumbwheel commands the system to hold the existing inertial velocity.

Simulation Experiment

Simulator Facility

This experiment was conducted on the Vertical Motion Simulator (fig. 7) at Ames Research Center. The simulator provides six degree-of-freedom motion that permits particularly large excursions in the vertical and longitudinal or lateral axes. Bandwidths of acceleration in all axes, including pitch, roll, and yaw, encompass the bandwidths of motion sensing that are expected to be of primary importance to the pilot in vertical flight tasks. The cockpit longitudinal axis was oriented along the motion system's translational beam to exploit the motion system authority based on the tasks in this experiment. Appendix A lists the simulator motion system performance as well as the motion washout filter characteristics adopted for this experiment.

An interior view of the cockpit is shown in figure 8. A three-window, computer-generated imaging (CGI) system provides the external view. The CGI could present an airfield scene or a ship scene, the latter modeling an LPH-type amphibious assault ship. A center stick and rudder pedal arrangement is seen in the figure, along with a left-hand throttle quadrant of the kind used in the Harrier. This quadrant contains both the power lever (throttle) and thrust vector deflection handle (nozzle lever). Overall frame time for output of the CGI in response to the pilot's control inputs was 0.065 sec, of which 0.015 sec was the host computer frame time.

Evaluation Tasks and Procedures

The pilot's operational tasks for evaluation during the simulation were (1) curved, decelerating approaches to hover, followed either by a vertical landing on the airfield or aboard the LPH, (2) accelerating transitions from hover to conventional flight, (3) short takeoffs, and (4) vertical takeoffs. Complete circuits from takeoff, accelerating transition to cruise flight, decelerating transition to hover, and vertical landings were also performed. For evaluation purposes, the decelerating approaches were divided into two phases. The first phase was initiated in level flight at 200 knots in the landing configuration. The aircraft's initial position was on a downwind heading abeam the initial hover station-keeping position. The sequence of events for the initial phase was capture of a 3 deg glideslope, commencement of a 0.1g nominal deceleration, turn to base leg and then to align with the final approach course, and, on short final at a range of 1000 ft, a change in nominal deceleration rate to 0.05g. Desired performance was defined as keeping the center of the ghost aircraft within the circular element of the flightpath symbol, with only momentary excursions permitted (analogous to 1/2 dot deflection on a standard instrument landing system display). Adequate performance was achieved when tracking excursions were significant, but not divergent. The initial phase of the approach was considered complete at the change in deceleration rate corresponding to the final closure to the hover point.

Acquisition of the hover 43 ft above the landing surface was the final phase of the approach. For the shipboard approaches, this included an initial station-keeping hover 100 ft to port and 100 ft aft of the landing spot, followed by a constant altitude translation to a hover over the landing pad. Desired performance was defined as acquisition of the hover with minimal overshoot and altitude control within ± 5 ft. Adequate performance was achieved when overshoot did not result in loss of the

landing pad symbol from the display field of view and altitude control was safe.

The vertical landing was accomplished on either a 100 by 200 ft landing pad on the runway or shipboard on Spot 5 1/2 located just aft of the island structure and 2/3 of the length of the deck from the bow of the LPH. Desired landing performance was defined as touchdown within a 5 ft radius of the center of the pad with a sink rate of 3 to 5 ft/sec. Adequate performance was considered to be touchdown within the confines of the pad at sink rates less than 12 ft/sec and with minimal lateral drift.

Slow landings and rolling vertical landings were performed under visual meteorological conditions (VMC) to the touchdown zone on the STOL runway. Initial approach path guidance was provided by the ghost aircraft up to the point where the pilot established the reference airspeed for the remainder of the approach. At that time, the pilot deselected approach path and deceleration guidance and aimed the flightpath symbol at the landing pad symbol on the HUD that overlaid the touchdown zone.

Accelerating transitions were initiated from the hover under VMC with full throttle and rotation of the thrust vector. The rate of thrust vector deflection was restrained to ensure a level to slightly climbing flightpath. The pilot chose the pitch attitude to achieve best acceleration. The transition was considered complete when the aircraft accelerated to 200 knots. In addition, waveoffs were executed at various points during the decelerating approach to permit the pilot to assess the transient control associated with conversion from the approach to an accelerating transition. The pilots' assessments of this task were based on the effort required to execute the transition within the constraints imposed above and the sensitivity of their performance of the task to abuses or variations from the recommended technique.

Short takeoffs were executed either from the runway or from the deck of the LPH. Takeoff procedures involved setting the stop for the thrust vector lever in accordance with the takeoff weight, setting full thrust and initiating the takeoff roll, accelerating to lift-off speed, moving the thrust vector lever to the takeoff stop, and rotating the aircraft to a pitch attitude of 10 degrees. Following lift-off, the aircraft was allowed to climb and accelerate; the pilot vectored the thrust aft while maintaining a positive rate of climb.

Vertical takeoffs were also carried out from the runway or LPH, initiated with the thrust vector lever at the hover setting of 85 deg followed by application of maximum thrust.

Two pilots with V/STOL aircraft experience acted as evaluation pilots in this experiment. Handling qualities ratings and commentary were obtained, based on the Cooper-Harper rating scale of reference 11.

Experiment Configurations

The experiment was carried out using the baseline aircraft described above. Approaches were conducted in instrument meteorological conditions (IMC) consisting of a ceiling of 100 ft and a visual range of 1200 ft in fog with varying winds, turbulence, and sea state. For operations to the runway, wind conditions of 0, 15, and 34 knots at 30 deg to the left of the final approach course and associated rms turbulence of 0, 3, and 6 ft/sec were used. Shipboard landings on the LPH were performed in sea states of 0, 3, and 5. Wind over deck was down the deck centerline at 10 knots in calm seas or 20 knots for the higher sea states. Approaches and landings were conducted to evaluate the baseline controls and displays, the switch of the throttle from thrust to flightpath and vertical velocity control and for specific variations from the baseline control laws and displays. Waveoff from the approach and transition to wing-borne flight provided an assessment of the switch of the throttle scaling from vertical velocity to thrust control and for the assessment of yaw control blending. Short takeoffs and vertical takeoffs followed by an accelerating transition to wing-borne flight enabled the evaluation of yaw control blending.

Variations in the controls and displays were associated with the vertical velocity command control law, the speed range over which the yaw stabilization and command augmentation law blended from sideslip command to yaw rate command, and the scaling of lateral displacement of the flightpath and ghost aircraft symbols on the HUD. The vertical velocity control law included two options, one that employed normal acceleration feedback and proportional plus integral control, and the second, which used only vertical velocity feedback and proportional throttle feed forward to achieve the vertical velocity command function. The intent was to determine the flying qualities for approach and landing of a simpler control law for the vertical axis than that used in the earlier simulation and flight experiments. Yaw control blending was performed either over a range from 40 to 60 knots or 40 to 100 knots ground speed. The effect of the blending is to increase directional stability (N_β) from zero at 40 knots to its nominal value ($N_\beta = 4$ rad/sec^2/rad) at the upper end of the blending region. Alteration of the lateral scaling for the flightpath and ghost aircraft symbols was accomplished by changing the scaling factor K_ε on flightpath and ghost aircraft crosstrack angle in

equations 173 and 178 of reference 9. This scale factor was either set at a nominal value of 0.3, as had been used throughout the previous simulations and VSRA flight program, or at a value of 1.0 to provide conformality of these symbols with the external scene. In either case, below 60 knots these two symbols no longer presented angular registration with the external scene and presented scaled vertical and lateral velocities and ghost aircraft crosstrack angle instead, as noted in reference 10.

Discussion of Results

Flying Qualities Assessment of Baseline Configuration

Evaluation of the baseline configuration provided a comparison of the pilot's assessment of flying qualities and measures of task performance for the various phases of operation associated with the STOVL flight envelope with previous assessments and measures obtained for the lift fan configuration in an earlier simulation (ref. 5). This comparison was made to identify any differences arising from the adoption of the full nonlinear inverse control laws. The discussions to follow cover the pilots' evaluations and representative performance and control usage measures for the separate phases of operation.

IMC Decelerating Transition– Handling quality ratings (HQR) for the baseline configuration for the various stages of the approach and landing are presented in figure 9. Ratings for the decelerating approach down to breakout to visual conditions at 100 ft are shown in figure 9(a). These ratings range from HQR 3 to 4 and reflect satisfactory flying qualities in calm air and light turbulence. A modest degradation to HQR 4 appears at the highest level of turbulence, indicating marginally adequate to satisfactory flying qualities under these conditions. Desired performance was achieved in all cases and only minimal compensation was required of the pilot in light winds and turbulence. A noticeable increase in compensation is apparent for the highest turbulence as a result of flightpath disturbances associated with the aircraft's moderate wing loading ($W/S = 57$ lb/ft^2). Results are comparable to those obtained in the previous simulation (ref. 5), where the range of those data appears in the figure as the open bars. These results indicate that, in an aggregate sense, changes in the control law structure to the full nonlinear inverse and the throttle control switching and scaling produce flying qualities equivalent to those of the previous control design.

Example time histories of the decelerating transition in APP mode in calm air and in turbulence are presented in figures 10 and 11. In calm air (fig. 10), glideslope capture is accomplished with a smooth nose-down pitch rotation and the deceleration is initiated with a single input from the thumbwheel. The deceleration proceeds smoothly and the throttle is advanced steadily to maintain the glideslope as wing lift is reduced. When the throttle reaches 60 percent at 137 sec into the run, flightpath command engages without an observable transient and functions for the remainder of the approach. The switch from flightpath to vertical velocity command at 60 knots is transparent to the pilot. Minimal glideslope error exists and the approach proceeds with little control activity required of the pilot. The control of thrust magnitude and deflection that underpins the decelerating transition is illustrated as well in figure 10. The approach mode is engaged around 90 sec with the resultant thrust vector already deflected manually to 30 deg. Immediately thereafter the pilot commands the start of the deceleration, and thrust transfer from the cruise nozzle to the lift fan and lift nozzles occurs coincident with their deflection from 45 deg. As the deceleration progresses, thrust is continually increased, first caused by the pilot's advance of the throttle, then as a result of the flightpath command control starting at 137 sec. Along with the thrust increase, the thrust deflection follows the longitudinal axis control law commanded by the thumbwheel. For all of this activity from the individual thrust effectors, the demands placed on the pilot are for the deceleration command with the thumbwheel and the advance of the throttle up to the 60 percent reference point. Lateral-directional control through the turn from downwind to the final approach path is shown at the end of figure 10. Localizer capture for the final approach occurs with a small overshoot and proceeds with minimal errors. Small bank angle excursions are used to maintain flightpath tracking of the ghost aircraft. Sideslip excursions are minimal.

In the example of an approach in 6 ft/sec rms turbulence with a steady wind of 34 knots (fig. 11), the excursions in flightpath and increased control activity are apparent. Early on in the approach, pitch attitude is actively employed to suppress flightpath excursions and track the glideslope. Throttle activity is evident as well, up to the point at 138 sec into the run when flightpath command engages. Beyond that point, attitude remains constant and throttle control activity diminishes noticeably while flightpath variations are reduced considerably compared to the initial stage of the approach. Glideslope excursions are minimal throughout. The basis for the improvement in flightpath control is illustrated in the traces of thrust response in figure 11. In contrast to the thrust variations prior to flightpath command control engage at 138 sec, the thrust activity to reduce flightpath disturbances once the system is engaged increases substantially in magnitude and frequency content. Prior to flightpath command engage the thrust response is directly associated

with the pilot's throttle inputs. Thrust deflection throughout the approach is a result of the longitudinal axis control of deceleration. Lateral-directional control in figure 11 shows excellent localizer tracking with increased roll control activity to keep the flightpath symbol aligned with the ghost aircraft.

Glideslope and localizer tracking performance at breakout to visual conditions at 100 ft altitude is presented in figure 12 for varying levels of turbulence. With two exceptions, glideslope and localizer errors are within 0.5 deg and in all cases within 0.8 deg at this point in the approach, with no relation to the magnitude of turbulence. It should be noted that 0.5 deg deviation corresponds to an 8 ft offset from the glideslope and a 13 ft offset from runway centerline at the position corresponding to 100 ft altitude. This accuracy of tracking performance is within the desired tolerances noted earlier and leaves the aircraft well positioned for the pilot to complete the approach to hover visually.

Hover Point Acquisition– Pilot evaluations of the final stage of the deceleration and acquisition of the hover are shown in figure 9(b). Fully satisfactory flying qualities were achieved with HQR falling between 2 and 3 in calm air and light turbulence. In the heaviest turbulence, ratings degrade slightly from HQR 3 to 4 as a result of a modest increase in pilot compensation to achieve the desired performance in arriving at the hover. Results correspond to experience in previous simulations. Time histories of figures 13 and 14 corroborate the ease of performing this phase of the approach. In calm air (fig. 13), the altitude and position capture proceed smoothly with gradual adjustments of the throttle and thumbwheel. Associated thrust response appears at the end of figure 13. In the presence of 6 ft/sec rms turbulence and the 34 knot quartering wind (fig. 14), somewhat more thumbwheel control activity is used to close to the hover point, and the altitude is undershot slightly. Thrust control activity to hold the hover height and thrust vector angle variations to adjust the arrival at the hover are also presented in figure 14. Substantial thrust variations are used to maintain the commanded vertical velocity in the presence of jet-induced lift disturbances associated with the varying wind.

Vertical Landing– Assessments of the vertical landing appear in figures 9(c) and 9(d) for runway and shipboard recovery, respectively. Runway landings are accomplished with fully satisfactory ratings regardless of the level of turbulence. The ease and precision with which the landing could be performed even led one pilot to a rating of HQR 1. No comparable data are available from the simulation of reference 5. For landings aboard the LPH assault ship, ratings were fully satisfactory in calm seas (HQR 1 to 3) and degraded slightly to borderline satisfactory (HQR 3 to 4) in the heaviest seas. Results once again compared favorably to the previous experience. The pilots' comments for the highest sea state centered solely on their effort to control sink rate relative to the deck for landing. Time histories for runway landings in calm air and in 6 ft/sec rms turbulence appear in figures 15 and 16. Landings in calm air (fig. 15) illustrate the ease with which the maneuver is performed. The aircraft moves forward to the landing position and the pilot makes a single throttle input to establish the desired rate of descent. This situation is maintained until touchdown, at which point the throttle is further retarded to set the aircraft firmly on the runway. Figure 15 also shows the thrust activity to hold the sink rate in the presence of ground effect, particularly the substantial increase in thrust to counter significant suckdown and thrust transfer from the lift nozzles to the lift fan in reaction to the change in jet-induced pitching moment. This compensation comes from the nonlinear inverse element of the vertical axis control law. The task is accomplished with the same simplicity of control in turbulence (fig. 16) as in calm air. The aircraft is established in position over the landing spot and the landing sink rate is set up with a reduction in the throttle with no further inputs until touchdown occurs. Thrust control activity in response to perturbations in lift due to winds and ground effect is shown at the end of figure 16. Touchdown precision for runway and shipboard landings is presented in figures 17 and 18. Most of the touchdowns in figure 17 were within 5 ft of the center of the landing zone, with three exceptions which ranged from 7 to 12 ft aft of the spot. Turbulence or sea state had no appreciable influence on the results. In figure 18(a), touchdown sink rates were mostly less than the maximum target of 5 ft/sec, although a few exceedances as high as 7 ft/sec were observed in the presence of turbulence or sea state.

Slow Landing– Slow and rolling vertical landings were conducted to observe control system performance under these conditions. No formal flying qualities evaluations were obtained; however, an example of a slow landing approach to touchdown is included in figure 19 to illustrate the pilot's actions to accomplish the task. As with the previous examples, glideslope capture is performed by lowering the nose to establish the desired descent angle. The deceleration is initiated with the thumbwheel input. When the aircraft slows to the intended final approach speed, the thumbwheel is centered and the approach proceeds at the final stabilized airspeed, which in this example is 62 knots. Throttle activity to track the approach path to the initiation of the landing flare is minimal once flightpath command engages. Prior to this point, the throttle is advanced to increase jet lift as wing

lift diminishes. The throttle is advanced slightly prior to touchdown to arrest the sink rate and is then retarded following the landing. This same general procedure is followed for other slow or rolling vertical landings with the reference approach speed being the principal variable.

Short Takeoff– A representative heavy weight short takeoff is illustrated in figure 20. At the selected speed of 85 knots, the pilot moves the nozzle lever rapidly to the takeoff stop at 58 deg and raises the nose to capture the target pitch attitude. As the nozzle lever is moved to the stop, thrust is transferred from the cruise nozzle to the lift nozzles and energy is simultaneously transferred to the lift fan to generate lift for takeoff. Once a climb rate is established and the aircraft is accelerating to wing-borne flight, the pilot gradually moves the nozzle lever forward to reduce lift fan and lift nozzle thrust as wing lift increases and to generate more cruise nozzle thrust for added acceleration. Lift-off from the runway is smooth and the climb is established without difficulty.

Accelerating Transition– An accelerating transition from hover to wing-borne flight is shown in figure 21. After increasing thrust above the hover setting to establish a climb, the pilot moves the nozzle lever forward to initiate the acceleration without moving it so abruptly as to cause the aircraft to settle. As speed increases, the nose is raised to a climb attitude while the nozzle lever is advanced fully forward. As the nozzle lever is moved to deflect thrust, the lift fan and lift nozzles rotate to the aft position, then thrust transfer to the cruise nozzle proceeds. The pilot's control technique is uncomplicated and there was no difficulty noted in performing the transition.

Control Utilization–

Pitch control: Results of pitch control usage for the approach to landing are presented in figure 22. Data are broken out for the decelerating approach, hover point acquisition, and vertical landing, the latter either on the runway or aboard ship. The data indicate the maximum and minimum control used during each individual run for the respective flight phase. Mean values that represent the control used for trim during the run are also shown. The increment between the maximum or minimum and the mean value is an indication of the control used for maneuvering or counteracting external disturbances. For the decelerating approach (fig. 22(a)), peak control variations about the mean in calm air or light turbulence are on the order of 0.15 rad/sec^2, and increase to 0.2 rad/sec^2 in the heaviest turbulence. During the hover point acquisition (fig. 22(b)), slightly lower levels of control are used except for the highest turbulence, which shows peak control about the mean comparable to that for the approach. Runway landings (fig. 22(c)) exhibit control excursions about half those for the approach, and shipboard landings (fig. 22(d)) use even less. Data for the approach and hover point phase are comparable to the results obtained for this lift fan configuration in reference 5; however, the landing data of this experiment are substantially lower than those of references 2 or 5.

Roll control: Figure 23 includes results for roll control usage during the approach and landing. In this case, the data represent the peak excursion about the mean for each individual run and again are indicative of the control used for maneuvering and countering disturbances. Unless the aircraft is trimmed to hold sideslip against a crosswind, the mean roll control input is zero. In the decelerating approach (fig. 23(a)), peak usage in calm air ranges up to 0.18 rad/sec^2, and increases to 0.3 rad/sec^2 in light turbulence and to 0.6 rad/sec^2 in the heaviest turbulence. For the hover point capture (fig. 23(b)), the amount of control required is essentially double that for the approach across the range of turbulence. Runway landing data (fig. 23(c)) also reflects the sensitivity to increasing turbulence with control use up to 0.19 rad/sec^2 in calm air, increasing to as much as 1.39 rad/sec^2 in heavy turbulence. Peak control during shipboard landings (fig. 23(d)) is comparable to that for runway landings for calm air and seas and increases to 0.6 rad/sec^2 in the heaviest sea condition. These control use data compare to previous results of reference 5 for the approach phase and for the hover point and landing in calm air and seas. However, they are substantially greater in peak use for the hover point acquisition in heavy turbulence and fall within the lower range for the shipboard landing in heavy seas.

Yaw control: In figure 24, results are presented for yaw control use for all flight phases in terms of peak excursions from the mean. Data for the decelerating approach (fig. 24(a)) reveal a steadily increasing trend with turbulence level from 0.04 rad/sec^2 in calm air to 0.22 rad/sec^2 in the highest turbulence. During the hover point capture (fig. 24(b)), the amount of control use is roughly half that for the approach. Runway landing control levels (fig. 24(c)) are comparable to those for the approach, while levels for shipboard recovery (fig. 24(d)) are as much as 0.13 rad/sec^2 in the heaviest seas. Data for the approach are around 50 percent greater than those shown in reference 5 but are comparable for hover point acquisition and shipboard landing.

Modified Vertical Axis Control Law

A control law modification was made to determine the contribution to flightpath and vertical velocity command of state rate feedback and integral control in the vertical axis. This modification to the baseline control law removed the normal acceleration feedback and integral

control in the forward loop of the vertical velocity stabilization and command augmentation control law documented in figure 22 of reference 7. Only vertical velocity feedback and throttle control feed forward remained to provide the flightpath or vertical velocity command function. The result of this modification, which produced a simpler control law, was to alter the disturbance suppression at low and high frequencies while retaining the overall bandwidth of vertical velocity response to the pilot.

Results of the pilots' evaluations of this modification for the decelerating approach to a vertical landing indicated that, in comparison to the baseline configuration, inferior height control was observed in the presence of disturbances. Behavior in calm air was largely unaffected in comparison to the baseline. Flying qualities for the decelerating approach were similar to the baseline configuration for any level of turbulence. Ratings were HQR 2 to 3 in calm air and degraded mildly to HQR 3 to 4 in 3 ft/sec rms turbulence and up to HQR 4 in 6 ft/sec disturbances. For hover point acquisition, ratings were HQR 2 in calm air, HQR 3 to 4 in 3 ft/sec turbulence, and HQR 4 at 6 ft/sec. Thus the degradation with turbulence was somewhat more than for the baseline data shown in figure 9(b). Runway landings produced a more pronounced degradation in height control for the modified control law. While ratings in calm air were HQR 2 to 3, and in 3 ft/sec turbulence were HQR 2, in turbulence of 6 ft/sec the ratings worsened to HQR 4 to 5. Shipboard landings in sea state 5 produced ratings from HQR 3 to 6. The essence of the pilot commentary on height control in turbulence and for the highest sea state pointed to increased control activity to hold hover altitude and to establish and hold the desired landing sink rate. Demands for height control occasionally detracted from control of hover position. In some cases the desired hover precision could not be achieved. The conclusion from this investigation of this alternative vertical velocity command control law is that it leads to inferior flying qualities for the more demanding height control tasks in comparison to the control law which includes normal acceleration feedback and integral control. The latter remains the preferred control law for the vertical axis.

Throttle Control Scaling

In the course of the decelerating approach to hover, as the control mode is switched to flightpath control, and in the switch from APP or TRC to MTV mode to execute a waveoff or on touchdown, throttle scaling was switched between flightpath or vertical velocity command to thrust command and vice versa. These mode switches produced no transients in aircraft response that were observed by the pilots. An example of a switch from thrust to flightpath command during the approach is shown in figure 25. Throttle scaling for flightpath control appears at the top of the figure and represents a gradient that falls within the design limits of the control law in reference 7. The deadband of ±1 deg of throttle input around the position for level flight is noted at the upper right of the figure. Time histories of the command compared to aircraft response appear in the center diagram and are taken from the same approach to hover shown previously in figure 10. Actual flightpath tracks the command from the point of initial engage at 137 sec to the point at 60 knots (100 ft/sec) ground speed when the command changes from flightpath to vertical velocity. Beyond that point, vertical velocity follows the command input to the end of the segment where hover is established.

Two examples of the switch from flightpath (vertical velocity) to thrust command during the course of executing a waveoff from hover to the transition to wing-borne flight are presented in figures 26 and 27. In figure 26(a), command of thrust is initiated at a throttle position of 90 percent and thrust of 81 percent. As the pilot adjusts the throttle and eventually retards it to reduce thrust as the aircraft accelerates to higher speed, the gradient of thrust versus throttle is adjusted with each advance and reduction in the throttle until the nominal gradient of 1:1 is achieved. Time histories of this particular maneuver in figure 26(b) illustrate, respectively, the aircraft and propulsion system response to the mode switch and ensuing pilot commands. The time history begins at 235 sec in flightpath (vertical velocity) command mode followed shortly by a throttle advance to initiate a climb. Then the pilot selects MTV mode (with thrust command) at 240 sec and manually advances the nozzle lever to rotate the thrust vector aft to start the acceleration to wing-borne flight. No thrust transient occurs at this point; however, the thrust vector angle steps aft 3 deg to bring the actual vector angle into agreement with the nozzle lever command at the time of switchover. (Reference 7 indicates that the tolerance for the nozzle lever backdrive is within 3 deg of the thrust vector angle command.) Since the pilot moved the nozzle lever abruptly to the forward stop, the actual vector angle retraction takes place at the limited vector retract rate of 5 deg/sec. At this limited rate, without further intervention by the pilot, the rate of climb begins to reduce around 244 sec and the aircraft establishes a rate of sink due to the loss of powered-lift until the pilot adds thrust and raises the nose to reestablish the climb. By 252 sec into the run, the thrust command has adjusted to within the tolerance around the 1:1 slope. The second example of a mode switch (fig. 27) shows a different combination of throttle and thrust at the switch point. Following a large advance in throttle and

thrust to initiate the waveoff, the gradient adjustment takes place and the eventual throttle reduction proceeds along a slope within the range of tolerance about 1:1. In either of these cases, the response of thrust to throttle was acceptable to the pilot, who remained unaware of the adjustment in gradient.

Control Mode Blending

Assessments of yaw control mode blending to determine acceptable yaw transients as the aircraft accelerated through the blending region were made during the course of waveoffs from hover or during short takeoffs, in both cases in the presence of a 15 knot left crosswind. Example time histories of the yaw transients during an acceleration from hover are shown in figure 28(a) for the baseline configuration, and in figure 28(b) for the configuration with the blending region from 40 to 100 knots ground speed. The acceleration is nearly identical for the two cases. The aircraft begins the acceleration with the nose aligned with the runway centerline. Sideslip reduces with increasing ground speed up to 40 knots (68 ft/sec) where the blend from yaw rate command to sideslip command commences. Beyond that point, sideslip is reduced to zero at a rate commensurate with the increase in directional stability with speed. Comparing the two figures, it can be seen that the rate at which the nose swings into the wind for the alternate configuration is less than half that for the baseline configuration. The pilots found the baseline case to be objectionably abrupt, although not to the point of being disorienting. The alternate case was considered acceptable, even in poor visibility. During short takeoffs, the yawing characteristics after lift-off will depend on rotation speed, hence takeoff weight. Examples of the short takeoff for the baseline and alternate configuration are presented in figures 29(a) and 29(b) for a nominal rotation speed of 70 knots (120 ft/sec). For takeoff at this rotation speed, the benefit of the wider blending region was appreciated; whereas, for higher rotation speeds of 90 knots or more, the two blending configurations appeared similar to the pilot in terms of nose swing at lift-off.

Pitch control blending for the baseline configuration was performed over the speed range from 70 to 90 knots. This range was selected to correspond to the speed range over which wing lift becomes ineffective for control of flightpath. Above 90 knots, sufficient aerodynamic lift exists and vertical velocity damping is adequate for flightpath control through pitch attitude. In this case, the pitch rate command/attitude hold response type is appropriate for attitude control. Below 70 knots, aerodynamic lift has diminished significantly, the resultant thrust vector is deflected sufficiently, and thrust magnitude is at a level where thrust becomes the primary flightpath control. In this case, pitch attitude command is the best response type since the aircraft is normally set at a fixed pitch attitude for the remainder of the approach to hover. The pilots found this blending between the two response types to be smooth and free of any unwanted transients. Slow landings were typically conducted within the rate command range while rolling vertical landings were performed within the attitude command range. Operation within the blending range itself did not produce any objectionable attitude response.

Roll control blending for the baseline configuration was performed over the range from 40 to 60 knots. At speeds above 60 knots coordinated turns are desired, while below 40 knots lateral translation at a fixed heading is appropriate. Roll rate command is the desired response type with conventional turn coordination at higher speeds while attitude command provides the best handling for performing lateral translations at low speed. The pilots performed turns and sidestep maneuvers or turns over the speed range above, below, and within the blending region and found no inconsistent response to the lateral control.

Head-Up Display Conformality

The issue of registration of lateral guidance and control symbology against the external scene was assessed during the curved approach to a vertical landing in the presence of winds and turbulence. Flightpath and ghost aircraft scaling of 1:1 were evaluated in comparison to the baseline configuration which had scaling of 0.3:1. Scaling of 1:1 resulted in the flightpath and ghost aircraft symbols overlaying the external scene until the aircraft decelerated below 60 knots. From that point to the hover, scaling of the crosstrack angle for the ghost aircraft reduced from 1:1 to 0:1 proportionally with speed as described in reference 10. While the pilots appreciated conformality of flightpath and guidance symbols with the external scene during the approach, increased sensitivity of the symbols for lateral path tracking elevated the pilots' control activity, particularly in the presence of turbulence. Satisfactory tracking accuracy could be achieved with less control activity with the symbols scaled less than 1:1. The pilots preferred the choice of scaling (0.3) originally established for the display in the investigations of reference 10 and subsequently in the VSRA flight evaluations of reference 1. This preference was reinforced by the need in any event to scale the ghost aircraft crosstrack angle and to convert the flightpath symbol to scaled lateral velocity below 60 knots where angular relationships are inappropriate for lateral path tracking approaching the hover.

Conclusions

A moving-base simulation was conducted on the Vertical Motion Simulator at Ames Research Center using a model of an advanced, short takeoff and vertical landing lift fan fighter aircraft. Revisions were made to the flight/propulsion control system, head-up display, and propulsion system to reflect recent flight and simulation experience with STOVL operations. Objectives of the experiment were to evaluate (1) control law modifications over the low speed flight envelope, (2) integration of the throttle inceptor with flight control laws that provide direct thrust command for conventional flight, vertical and short takeoff, and flightpath or vertical velocity command for transition, hover, and vertical landing, (3) control mode blending for pitch, roll, yaw, and flightpath control during transition from wing-borne to jet-borne flight, and (4) effects of conformal versus nonconformal presentation of flightpath and pursuit guidance symbology on the out-the-window display for low speed STOVL operations. Assessments were made for takeoff, transition, hover, and landing, including precision hover and landing aboard an LPH-type amphibious assault ship in the presence of winds and rough seas.

No objectionable flying qualities were observed for the configurations tested, and Level 1 pilot ratings were obtained for the flightpath and vertical velocity command modes for a range of land-based and shipboard operation. These results compared favorably with earlier evaluations of this STOVL concept where control laws based in part on state-rate feedback implicit model following and different throttle scaling had been applied. An alternative vertical velocity command control law that used only vertical velocity feedback produced inferior flying qualities for demanding height control tasks in comparison to the baseline control law, which included normal acceleration feedback and integral control. The latter remains the preferred control law for the vertical axis.

The pilots were unaware of switching of the throttle between flightpath and thrust command functions. Blending of pitch control from rate command/attitude hold in wing-borne flight to attitude command/attitude hold in jet-borne flight was most successfully accomplished over a range of speeds where control of flightpath with attitude becomes ineffective. Blending of roll control from rate command/attitude hold to attitude command/attitude hold was performed over a speed range where turn coordination in wing-borne flight transitions to lateral velocity translation in hover. Blending of yaw control from heading command in hover to sideslip command in wing-borne flight was performed over a broad speed range to reduce abrupt yaw transients as the aircraft accelerates through the range in takeoff or transition flight.

While the pilots appreciated conformality of flightpath and guidance symbols with the external scene during the approach, increased sensitivity of the symbols for lateral path tracking elevated the pilots' control activity, particularly in the presence of turbulence. Satisfactory tracking accuracy could be achieved with less control activity with the symbols scaled less than 1:1, and the pilots preferred the choice of scaling (0.3) originally established during the display development and in flight evaluations. This preference was reinforced by the need to scale the ghost aircraft crosstrack velocity and to convert the flightpath symbol to scaled lateral velocity at low speed where angular relationships are inappropriate for lateral path tracking approaching the hover.

Pitch, roll, and yaw control utilization for maneuvering and disturbance suppression observed in this experiment was comparable in some respects and also showed some variance with previous simulation experience with this and other STOVL configurations. In particular, pitch control use was consistent with earlier simulations for the approach and hover point acquisition, while less control activity was noted for the landing. Roll control data compare favorably to previous results for the approach phase and for the hover point and landing in calm air and seas. However, they are substantially greater in peak use for the hover point acquisition in heavy turbulence. Yaw control data for the approach are greater than those of the earlier studies but are comparable for hover point acquisition and shipboard landing. These contrasts with previous simulation experience are presented as observations and are considered to reflect the variance in the results over a large number of samples. They are not felt to be attributable to specific features of the configuration or control system.

Appendix A

Vertical Motion Simulator Motion Characteristics

The Vertical Motion Simulator used in this experiment is capable of producing large translational and rotational motion cues over frequency ranges that encompass the bandwidths of control of the tasks associated with transition and vertical flight. Longitudinal, lateral, and vertical motion limits were ±20 ft, ±4 ft, and ±30 ft, respectively, with the cockpit longitudinal axis oriented along the main support beam. Translational motion system bandwidth (frequency for 45 deg phase lag) is 8 rad/sec for the vertical axis, 10 rad/sec for the longitudinal axis, and 20 rad/sec for the lateral axis. The rotational limits in pitch, roll, and yaw are ±18, ±18, and ±24 deg, respectively, and bandwidths are 10 rad/sec for each of the three axes. Motion drive logic for each axis commands accelerations through second order high pass (washout) filters that are characterized by their gain, natural frequency, and damping ratio. In all cases, damping ratios of 0.7 were used. Filter gains and natural frequencies are presented in table A1 for approach and hover tasks and for takeoff and accelerating transition tasks. Gains are blended between low and high speed flight conditions where the low speed region is below 20 knots and high speed is above 60 knots.

Table A1. Motion system gains and natural frequencies

Motion axis	Approach and hover case				Takeoff and transition case			
	Gain		Frequency, rad/sec		Gain		Frequency, rad/sec	
	Lo speed	Hi speed	Lo speed	Hi speed	Lo speed	Hi speed	Lo speed	Hi speed
Pitch	0.5	0.5	0.2	0.6	0.5	0.25	0.5	0.6
Roll	0.3	0.35	0.7	0.75	0.3	0.35	0.7	0.75
Yaw	0.5	0.5	0.2	2.0	0.5	0.5	0.2	2.0
Longitudinal	0.7	0.4	0.5	0.7	0.25	0.25	0.7	0.7
Lateral	0.5	0.5	0.7	2.0	0.5	0.5	0.7	2.0
Vertical	0.8	0.6	0.2	0.5	0.2	0.2	0.2	0.5

References

1. Franklin, J. A.; Stortz, M. W.; Borchers, P. F.; and Moralez, E.: Flight Evaluation of Advanced Controls and Displays for Transition and Landing on the NASA V/STOL Systems Research Aircraft. NASA TP-3607, Apr. 1996.

2. Franklin, J. A.: Criteria for Design of Integrated Flight/Propulsion Control Systems for STOVL Fighter Aircraft. NASA TP-3356, Apr. 1993.

3. Franklin, J. A.; Stortz, M. W.; Engelland, S. A.; Hardy, G. H.; and Martin, J. L.: Moving Base Simulation Evaluation of Control System Concepts and Design Criteria for STOVL Aircraft. NASA TM-103843, June 1991.

4. Franklin, J. A.; Stortz, M. W.; Gerdes, R. M.; Hardy, Gordon H.; Martin, James L.; and Engelland, Shawn A.: Simulation Evaluation of Transition and Hover Flying Qualities of the E-7A STOVL Aircraft. NASA TM-101015, Aug. 1988.

5. Chung, W. W. Y.; Borchers, P. F.; and Franklin, J. A.: Moving Base Simulation of an ASTOVL Lift Fan Aircraft. NASA TM-110365, Aug. 1995.

6. Franklin, J. A.; and Stortz, M. W.: Moving Base Simulation Evaluation of Translational Rate Command Systems for STOVL Aircraft in Hover. NASA TM-110399, June 1996.

7. Franklin, James A.: Revised Simulation Model of the Control System, Displays, and Propulsion System for an ASTOVL Lift Fan Aircraft. NASA TM-112208, Aug. 1997.

8. Birckelbaw, L. G.; McNeill, W. E.; and Wardwell, D. A.: Aerodynamics Model for Generic Lift-Fan Aircraft. NASA TM-110347, Apr. 1995.

9. Merrick, V. K.; and Jeske, J. A.: Flightpath Synthesis and HUD Scaling for V/STOL Terminal Area Operations. NASA TM-110348, Apr. 1995.

10. Merrick, V. K.; Farris, G. G.; and Vanags, A. A.: A Head Up Display for Application to V/STOL Aircraft Approach and Landing. NASA TM-102216, Jan. 1990.

11. Cooper, G. E.; and Harper, R. P., Jr.: The Use of Pilot Rating in the Evaluation of Aircraft Handling Qualities. NASA TN D-5153, Apr. 1969.

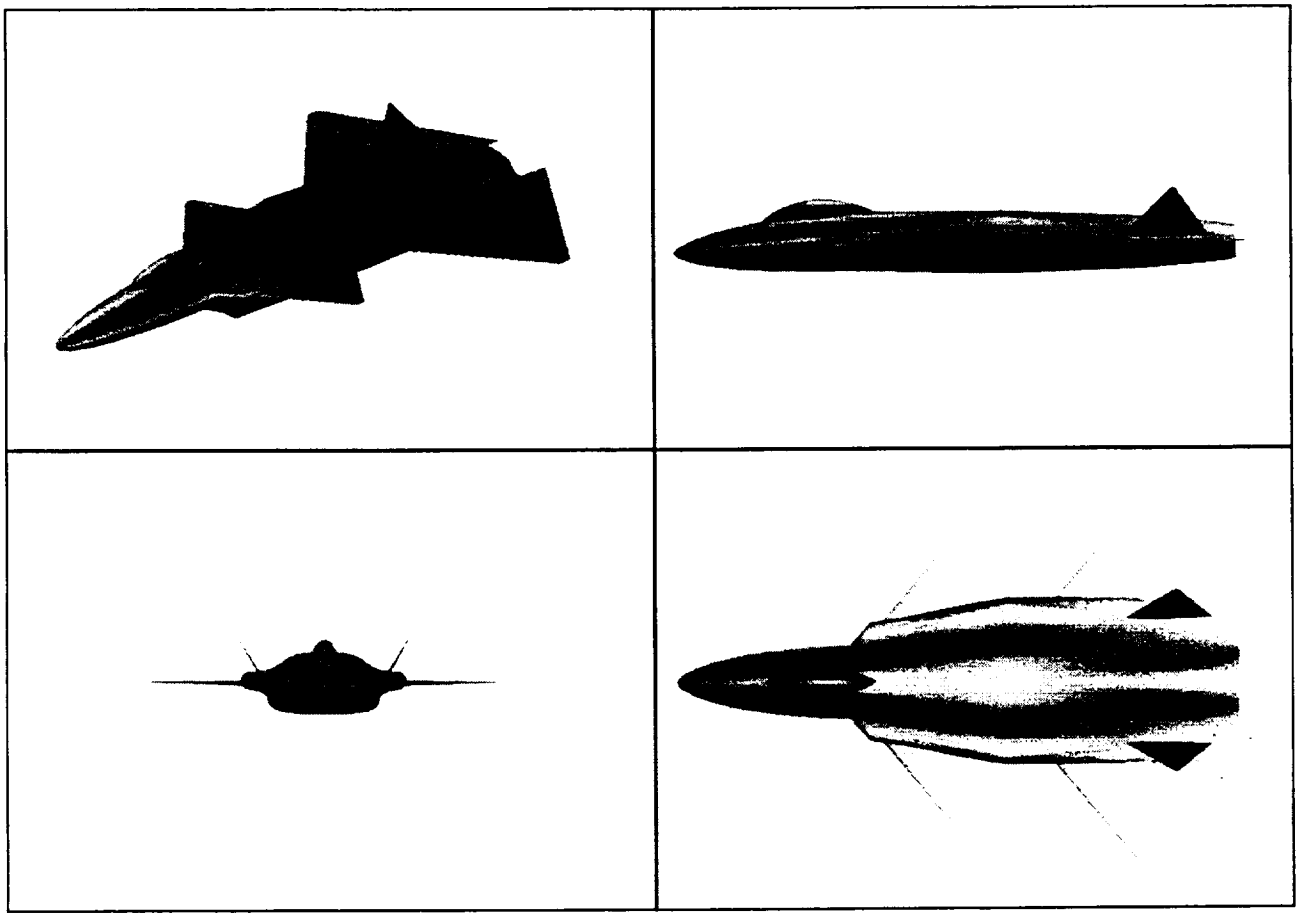

Figure 1. Views of the ASTOVL Lift Fan Aircraft.

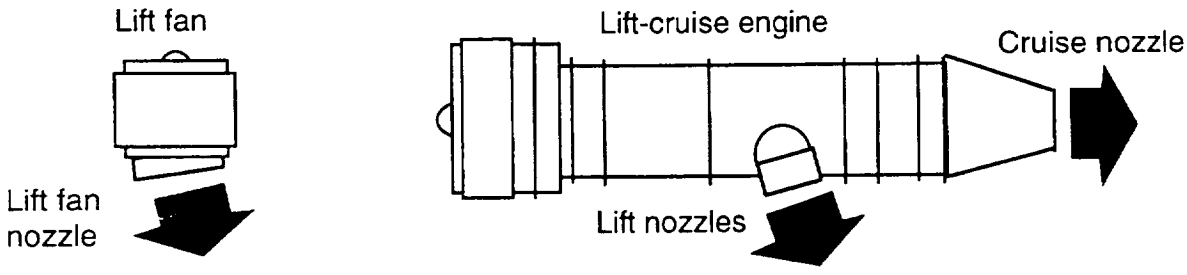

Figure 2. Propulsion system configuration.

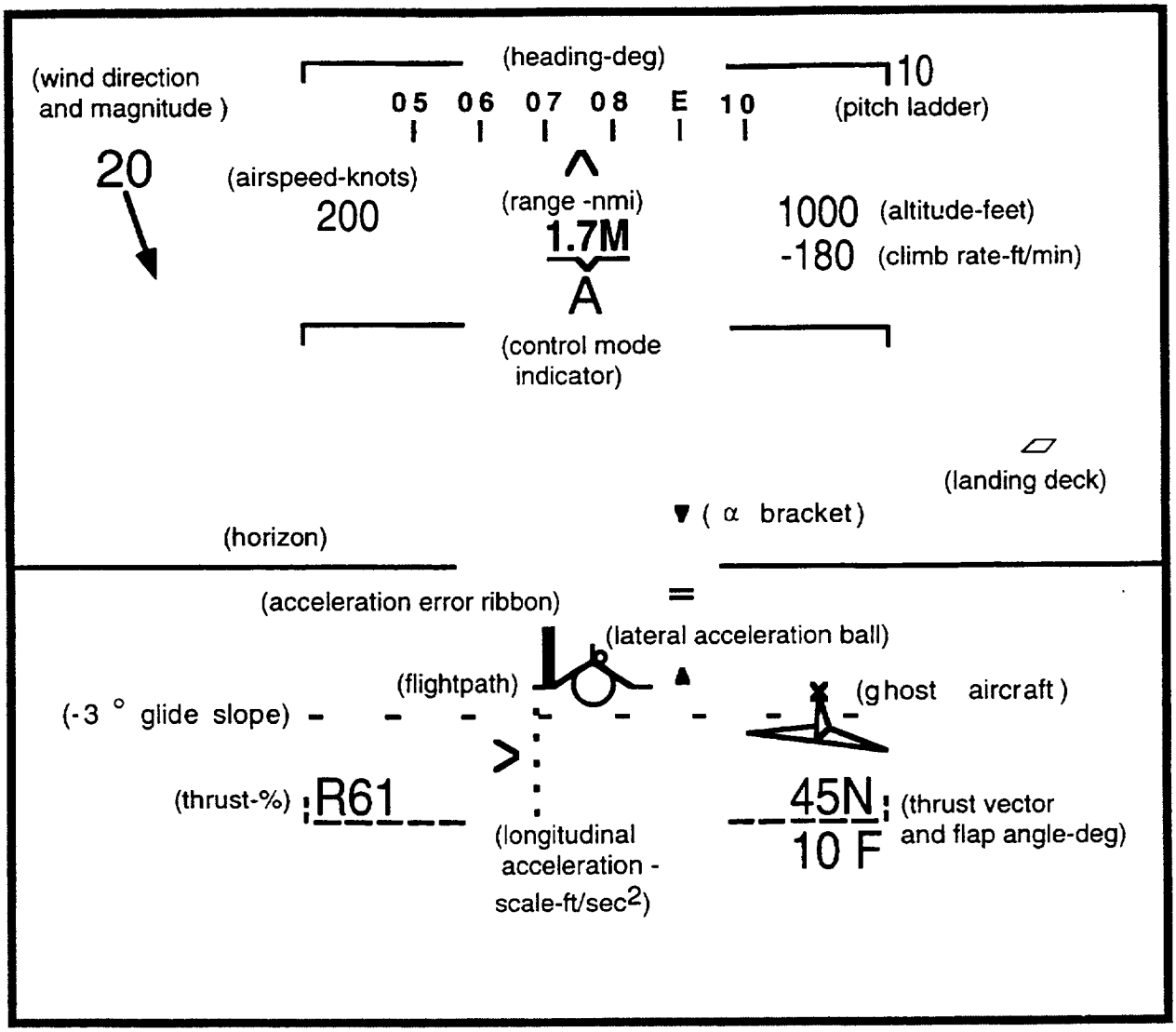

Figure 3. Approach display.

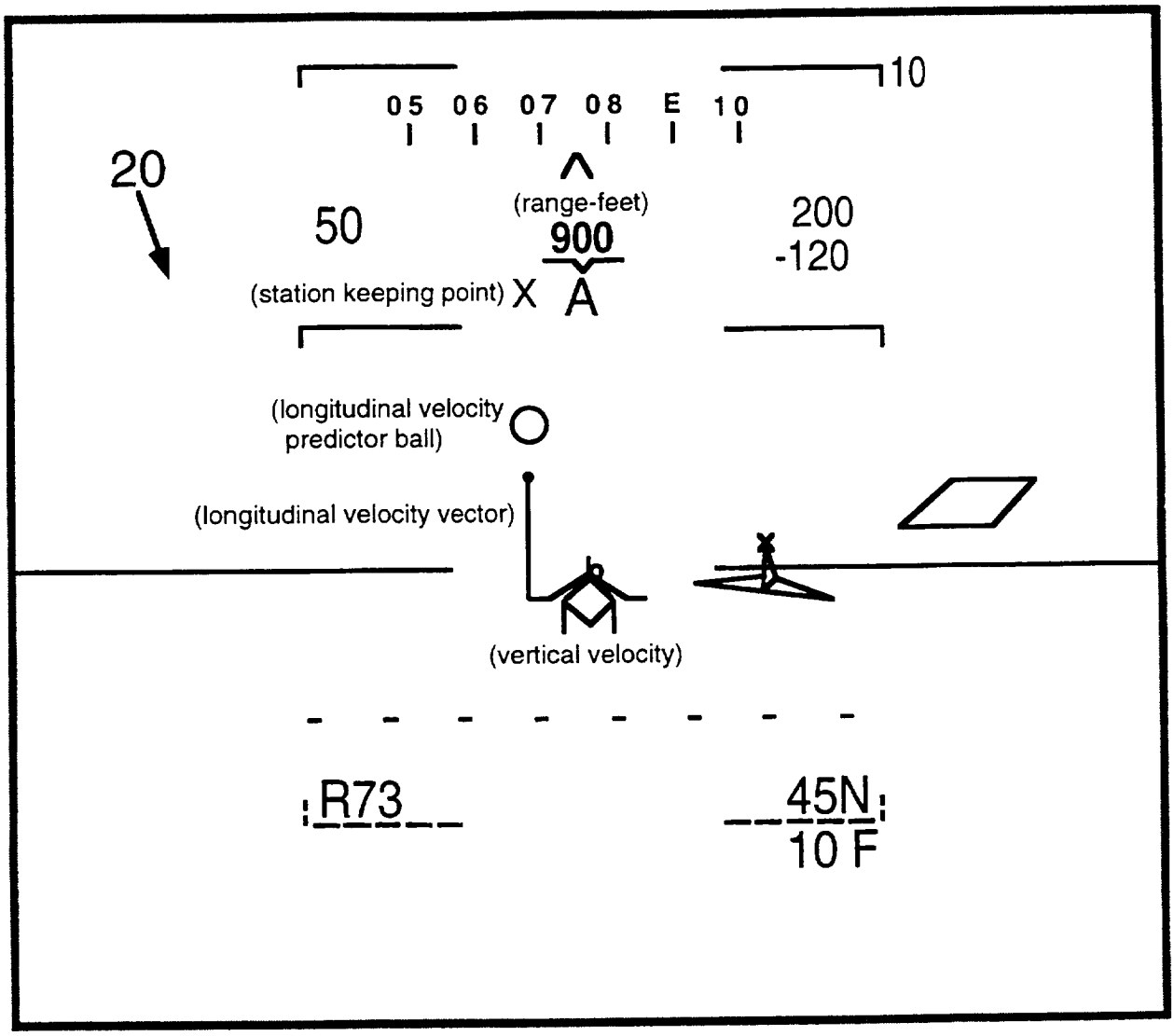

Figure 4. Symbology for station-keeping point capture.

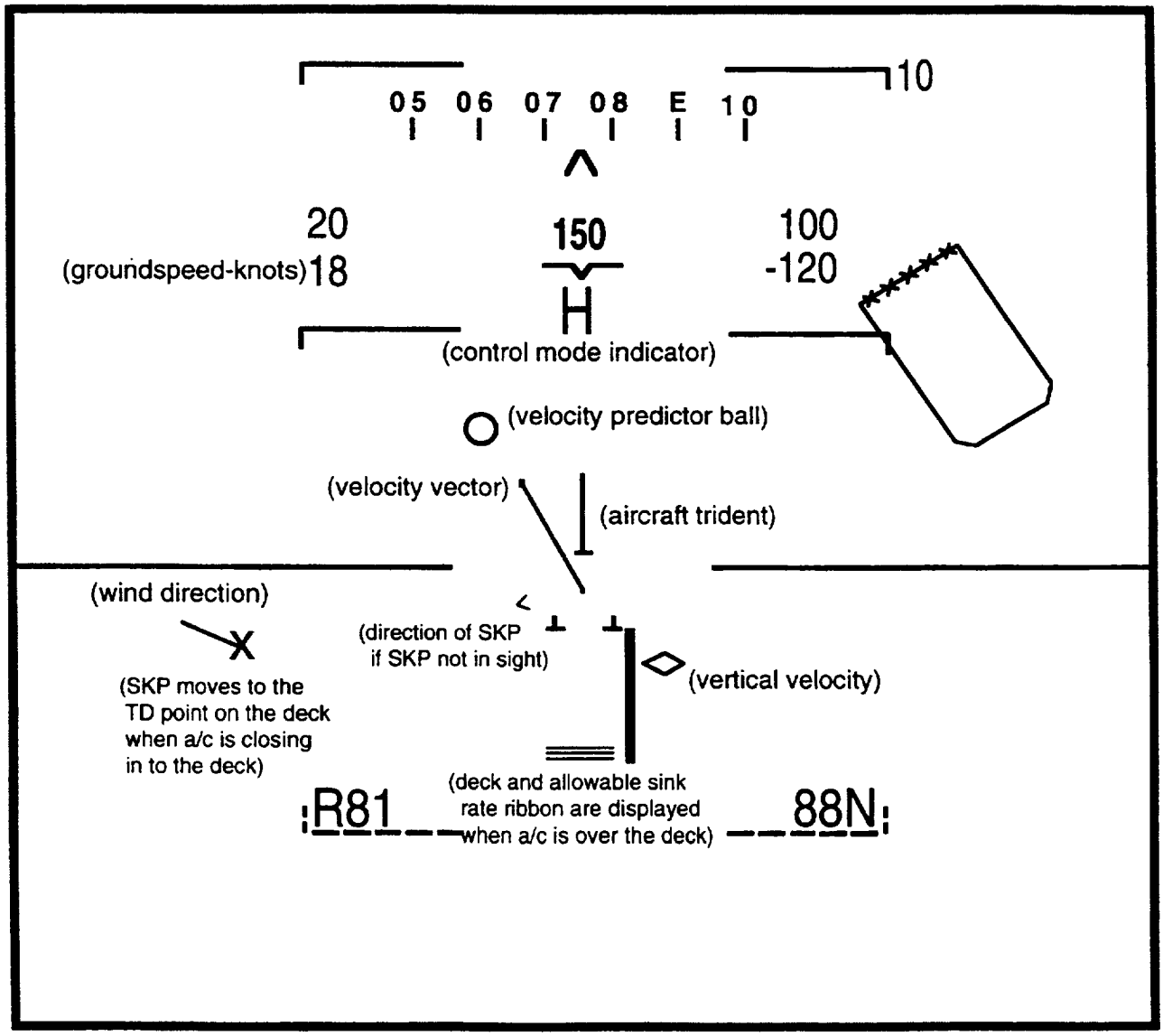

Figure 5. Hover display.

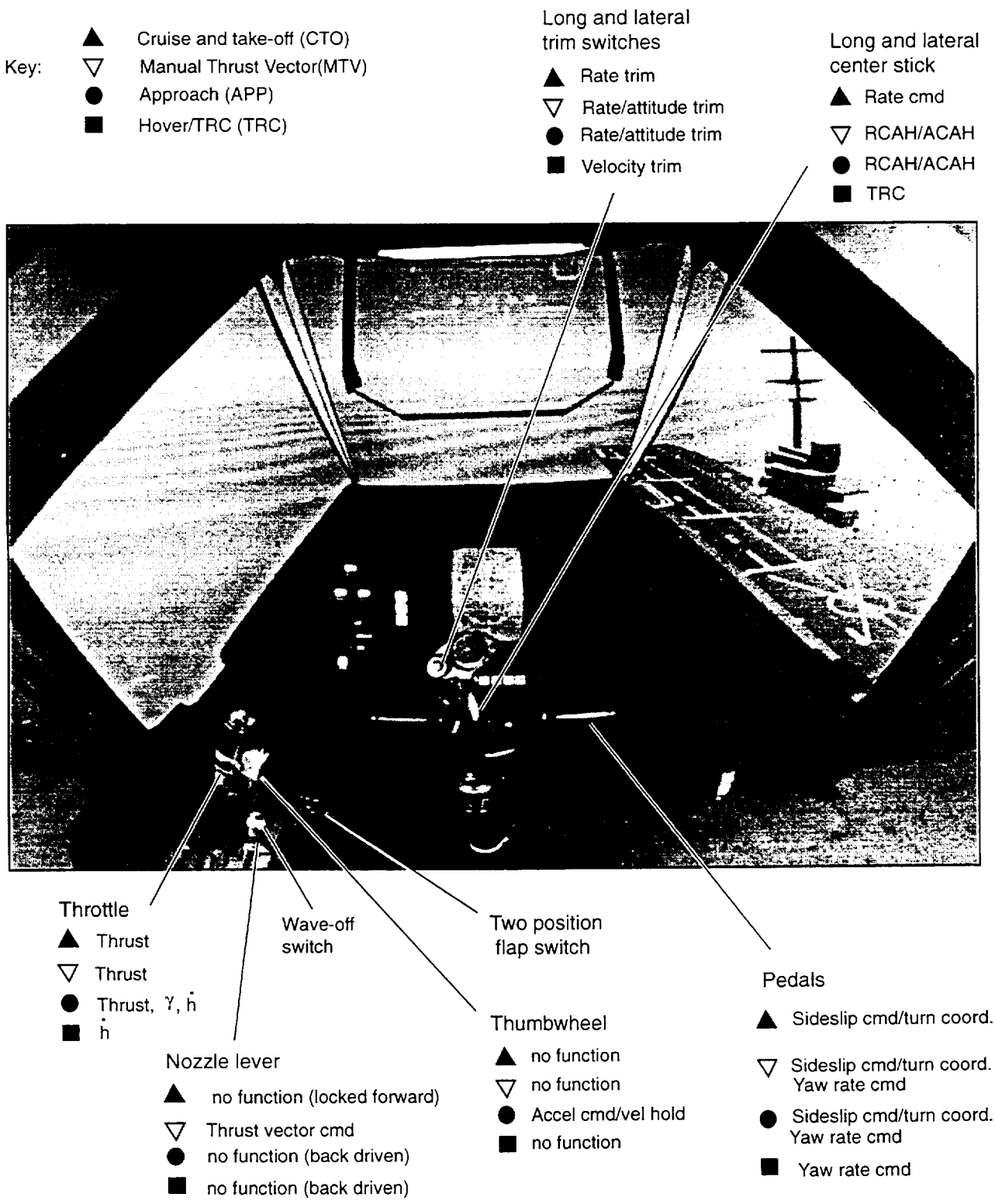

Figure 6. Inceptor functions.

VMS NOMINAL OPERATIONAL MOTION LIMITS			
Axis	Displ	Velocity	Accel
Vertical	±30	16	24
Longitudinal	±20	8	16
Lateral	±4	4	10
Roll	±18	40	115
Pitch	±18	40	115
Yaw	±24	46	115
All numbers, units in ft, deg, sec			

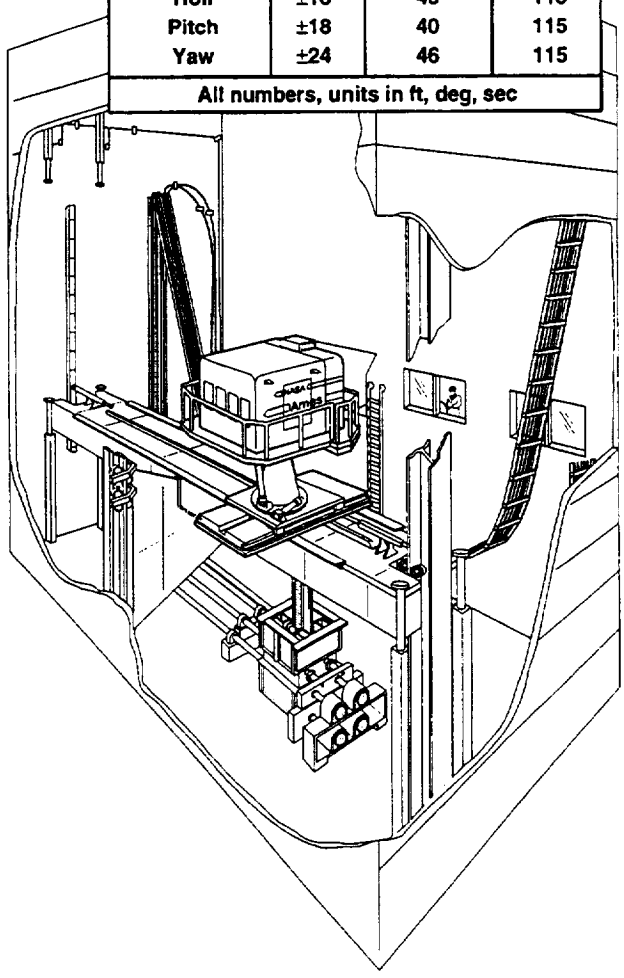

Figure 7. Vertical Motion Simulator.

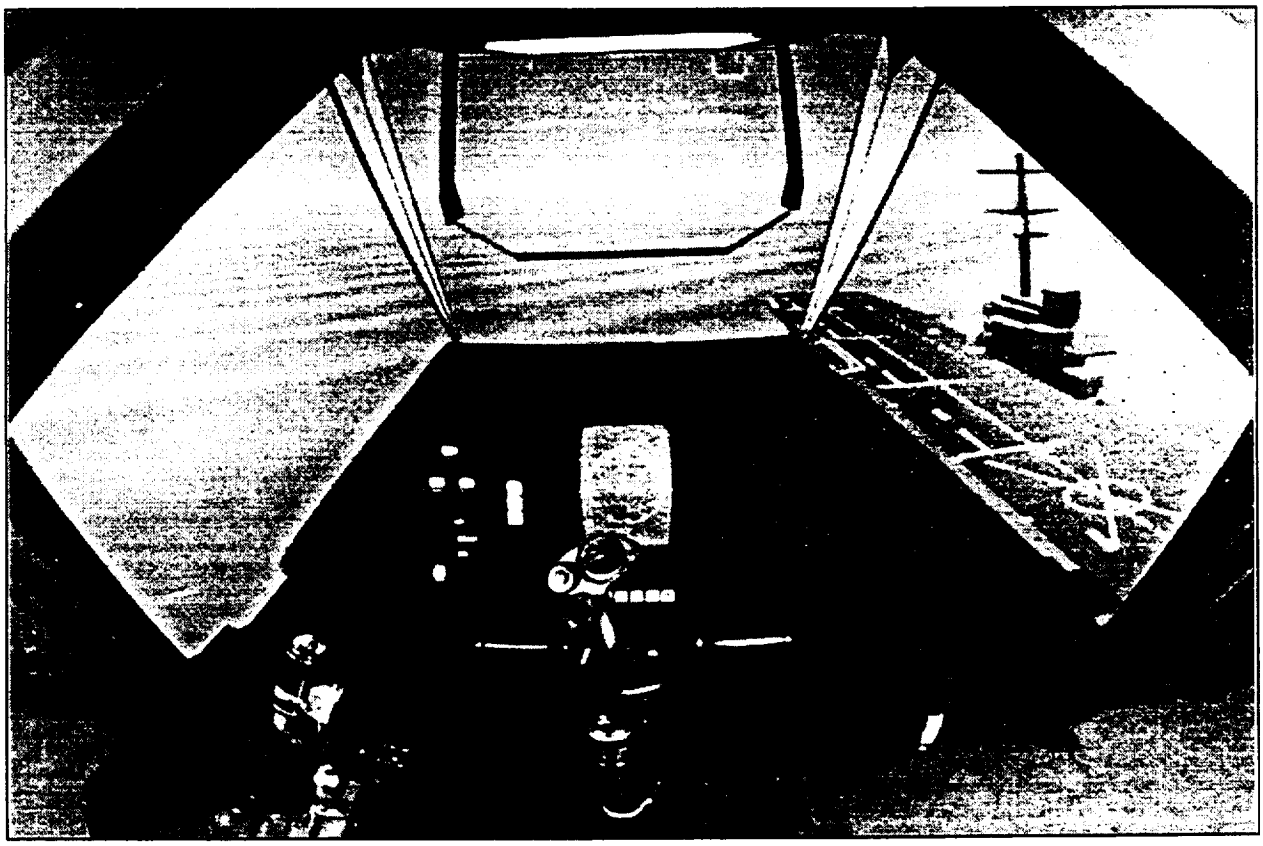

Figure 8. Simulator cockpit interior view.

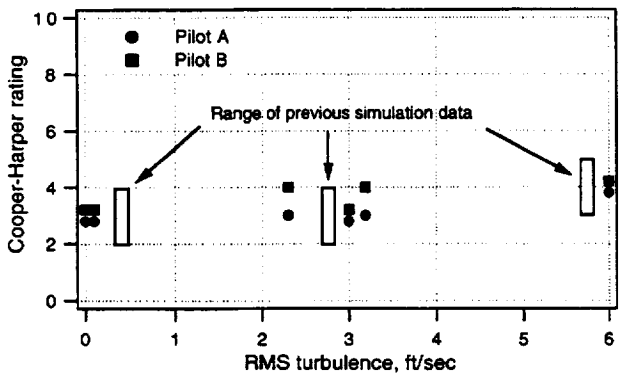

(a) Decelerating approach

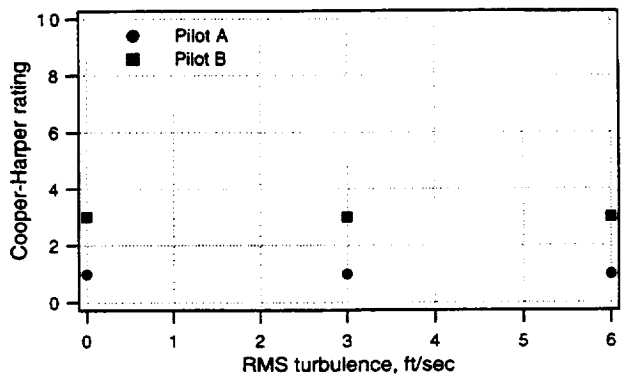

(c) Runway landing

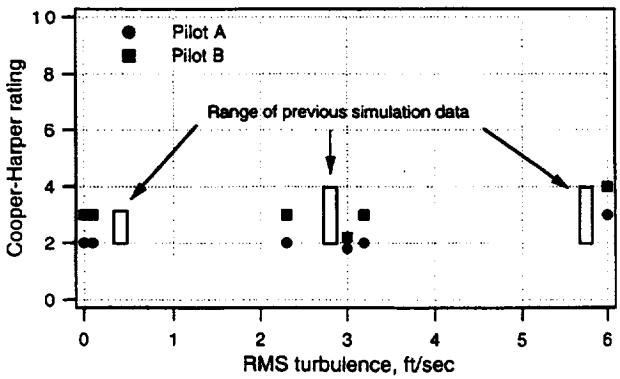

(b) Hover point acquisition

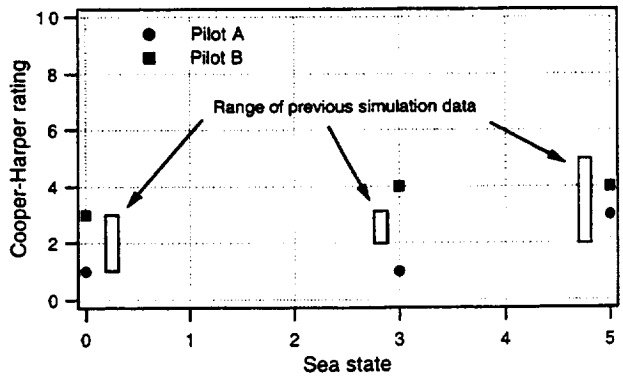

(d) Shipboard landing

Figure 9. Handling quality ratings for approach and landing tasks.

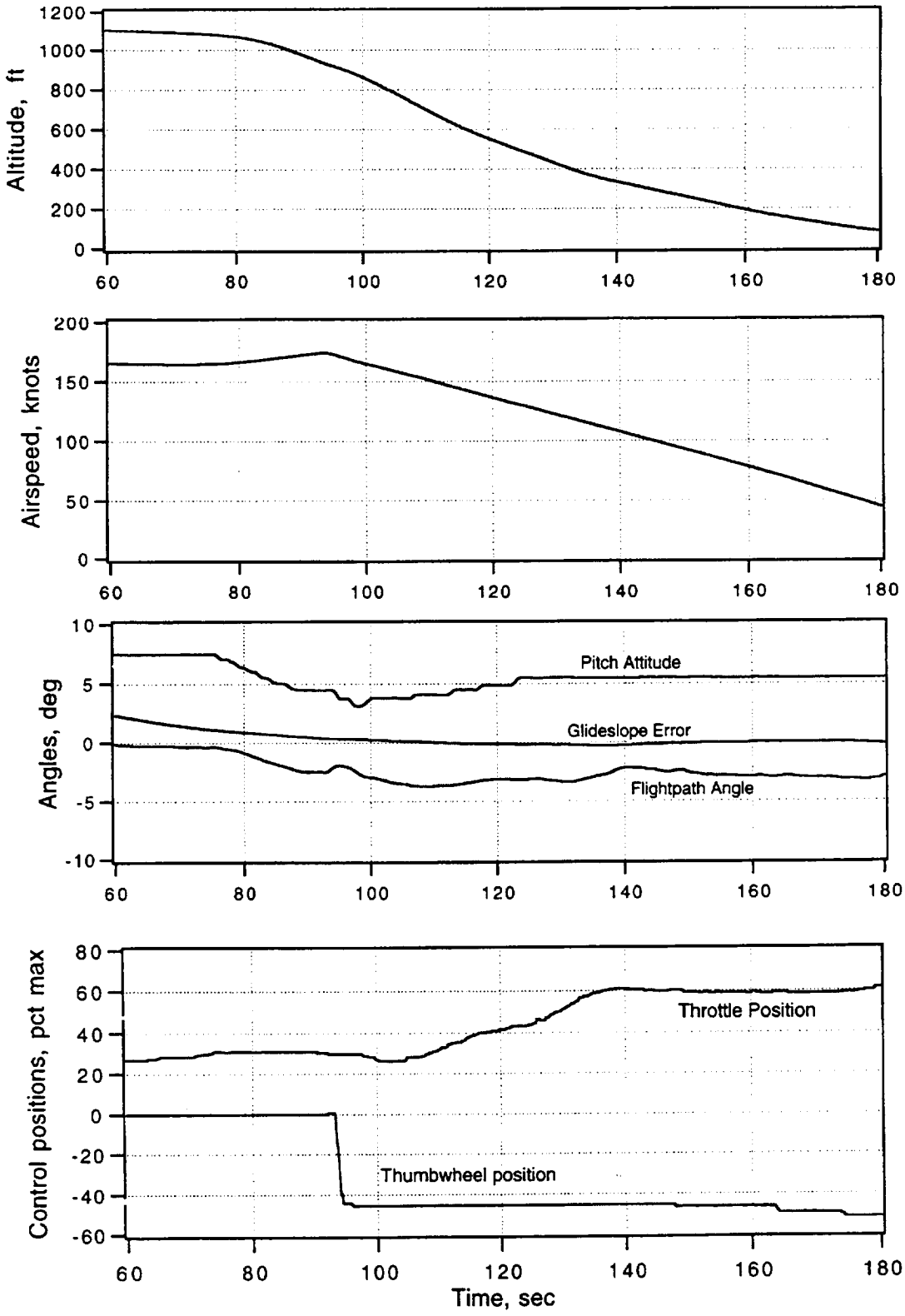

Figure 10. Time history of decelerating transition in calm air.

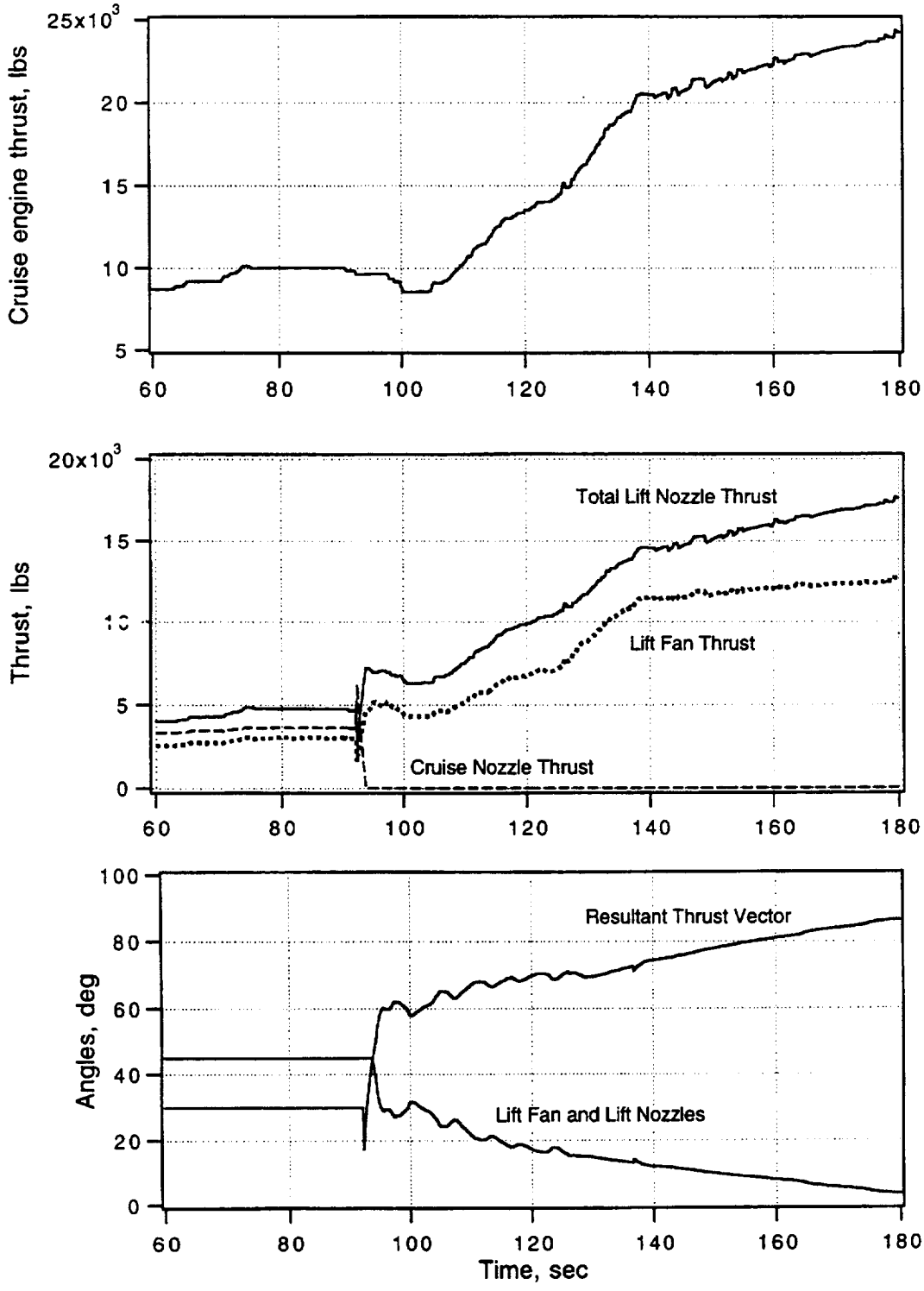

Figure 10. Continued.

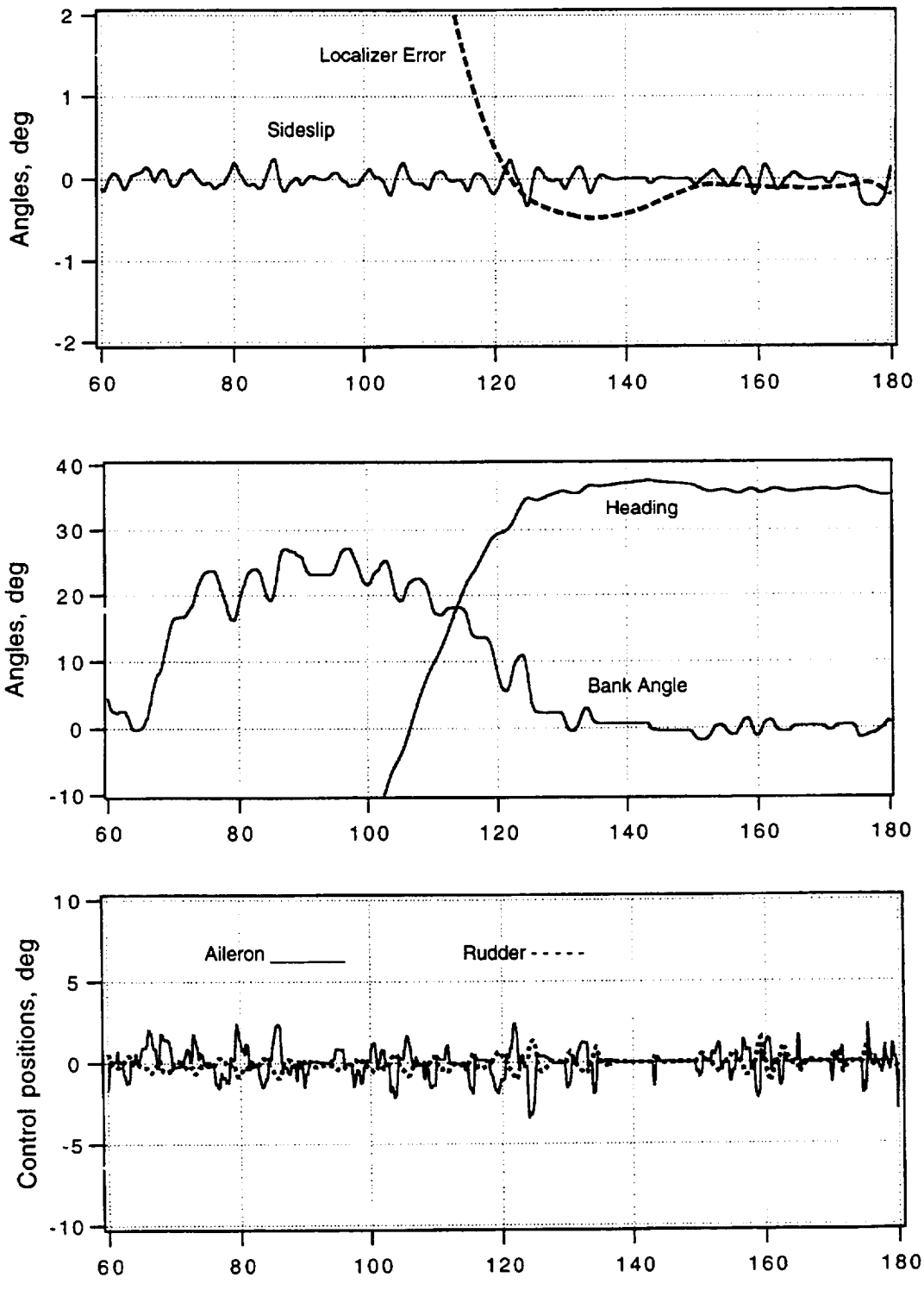

Figure 10. Concluded.

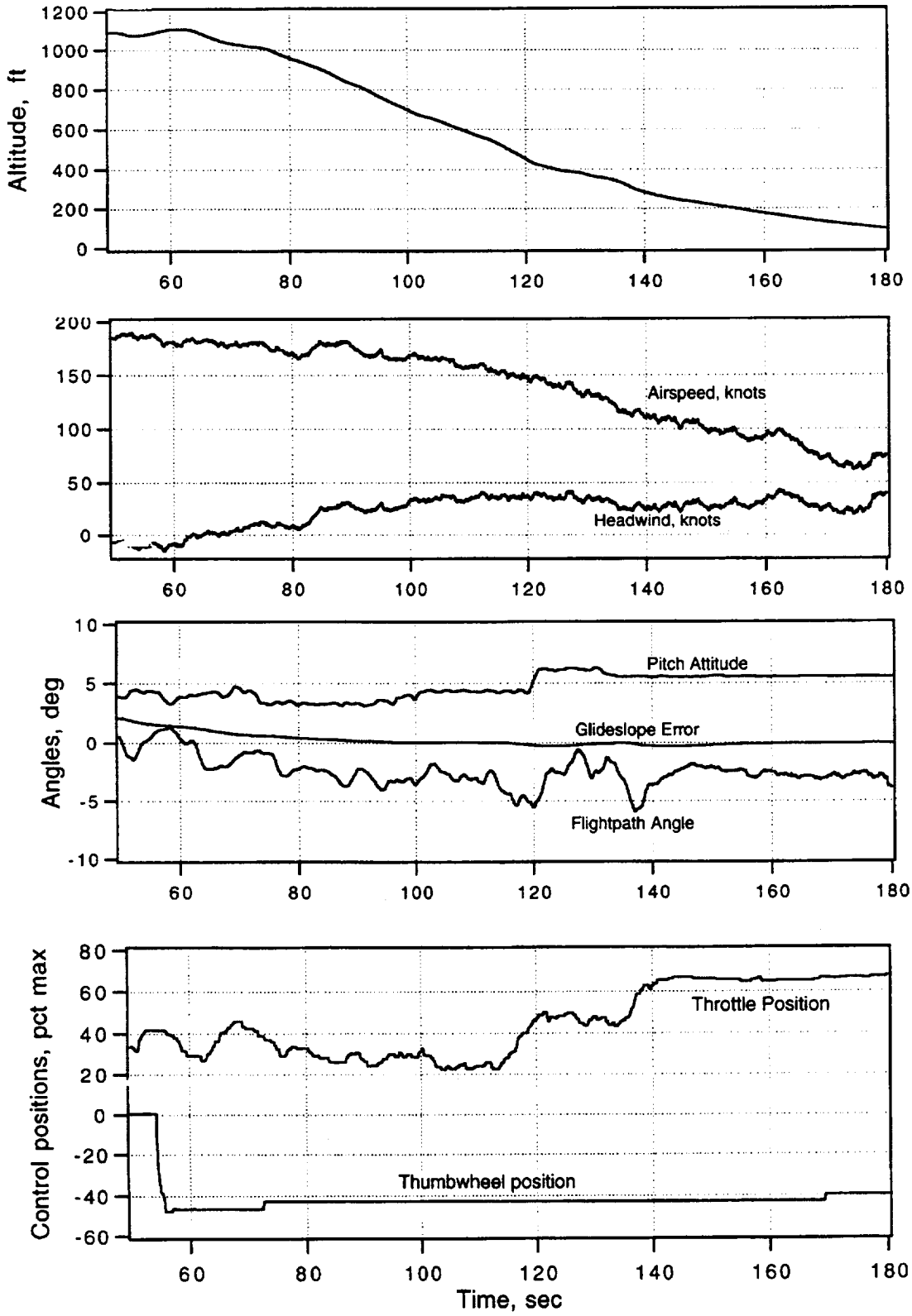

Figure 11. Time history of decelerating transition in 6 ft/sec rms turbulence.

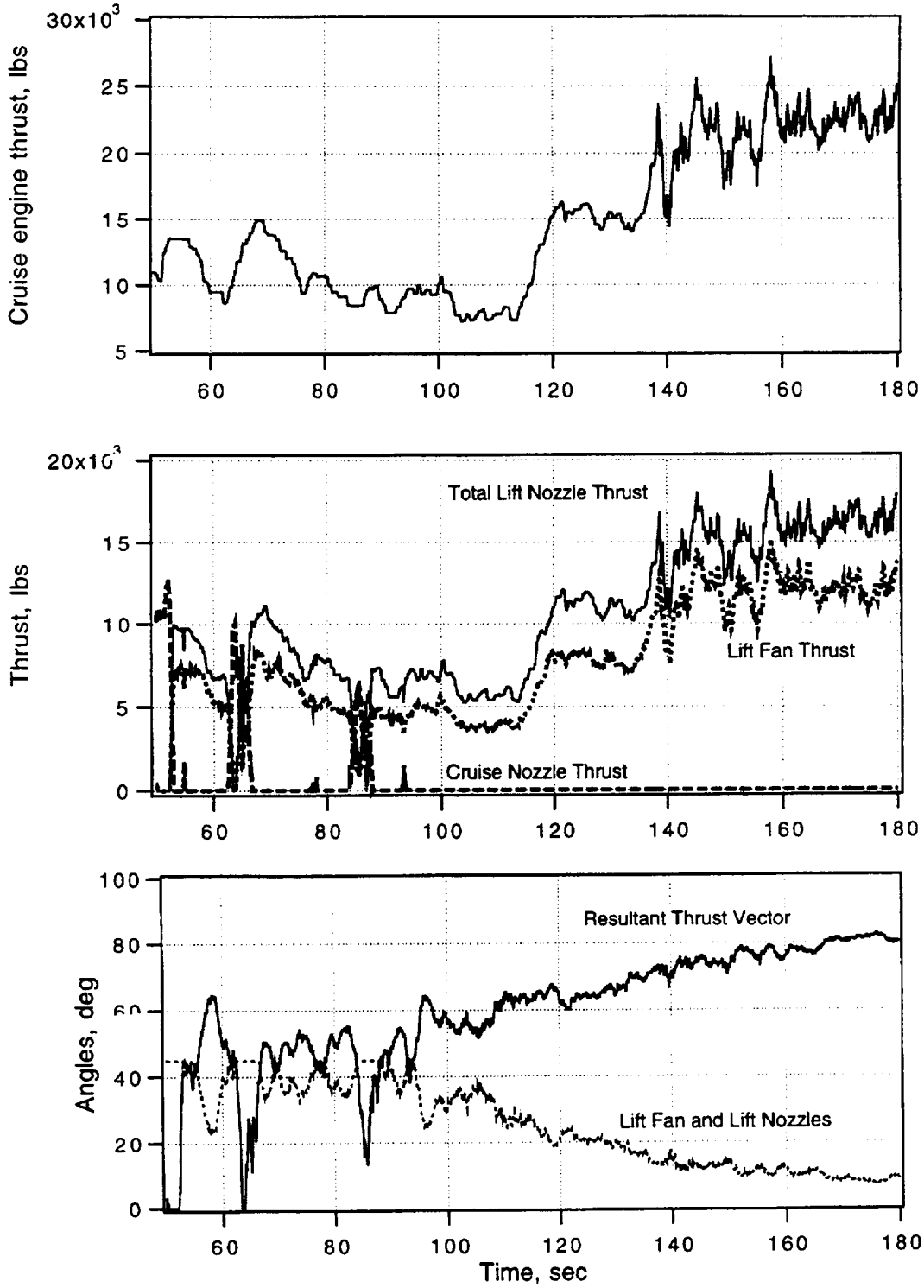

Figure 11. Continued.

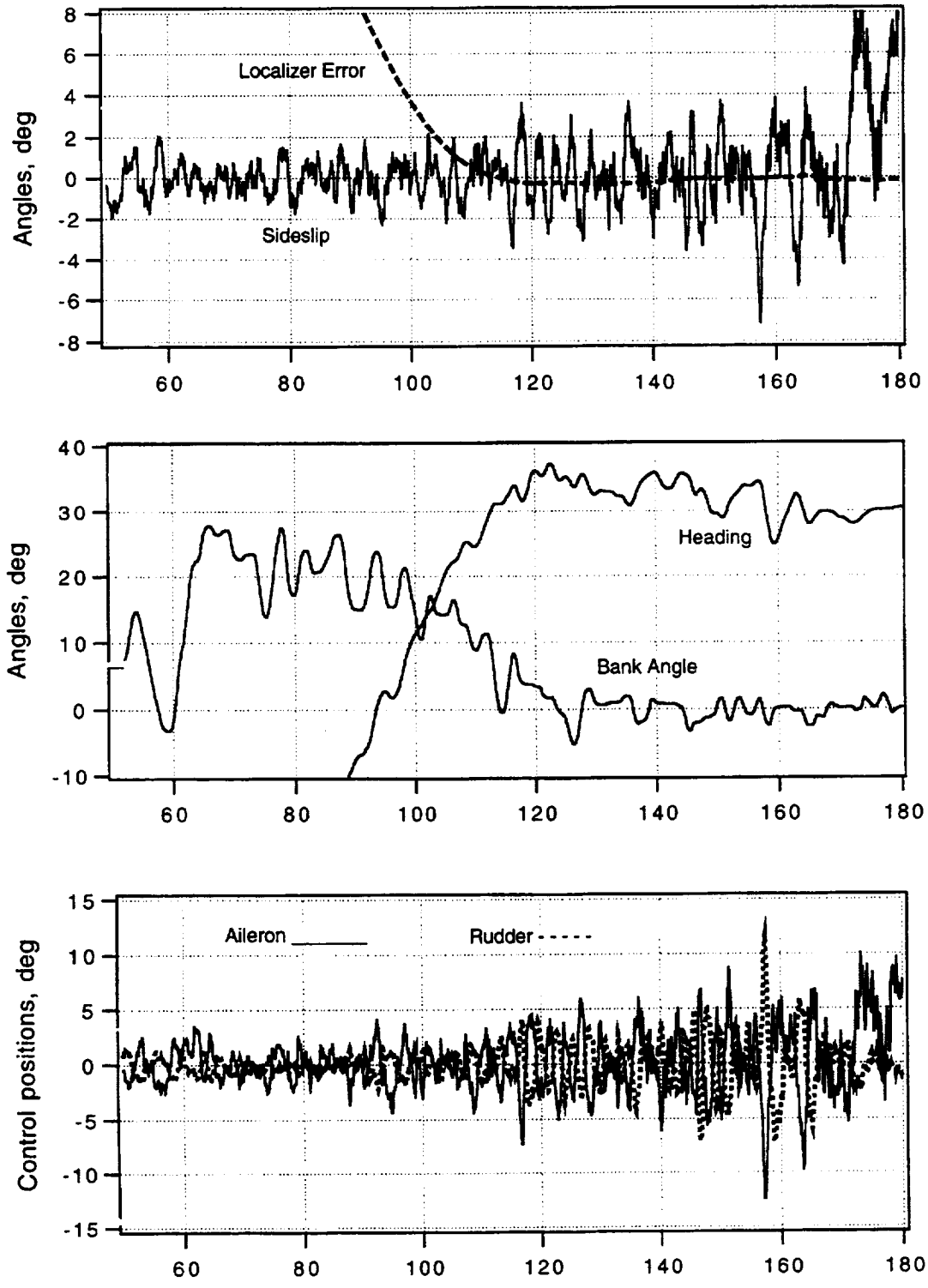

Figure 11. Concluded.

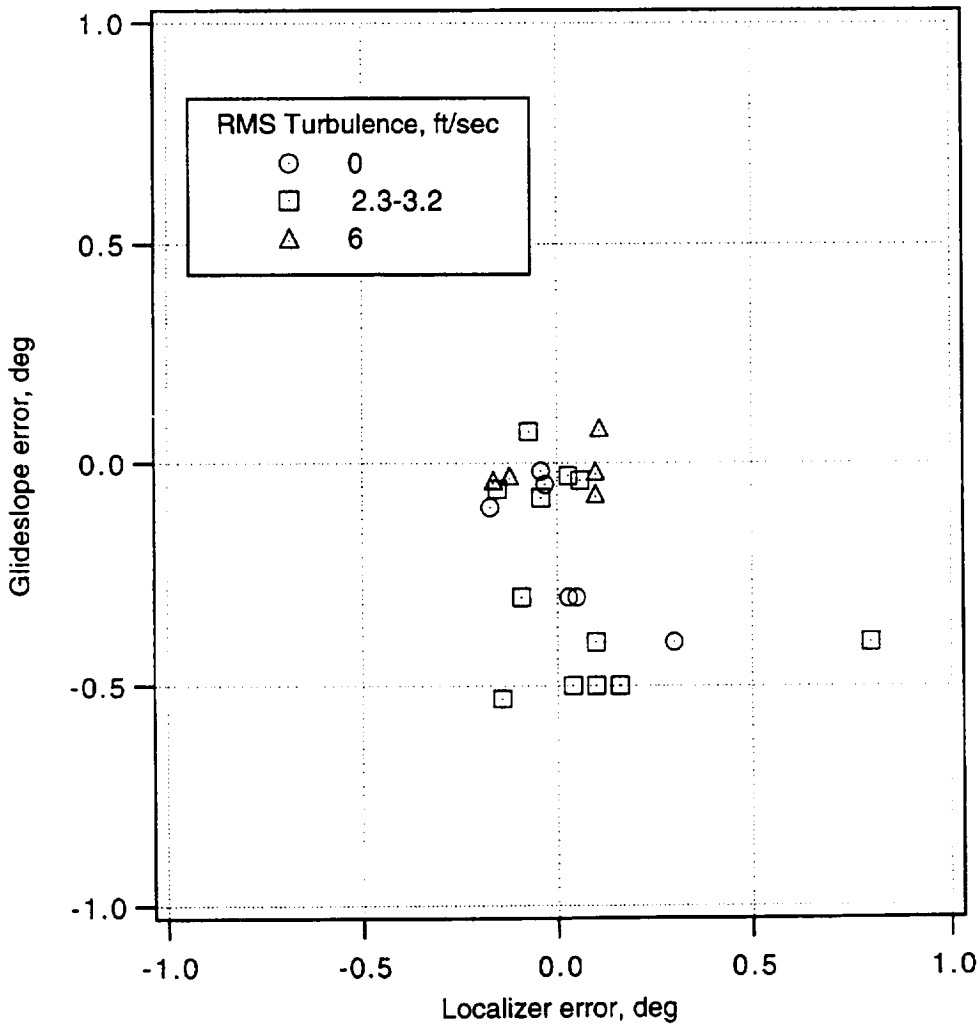

Figure 12. Glideslope and localizer errors at breakout altitude of 100 ft.

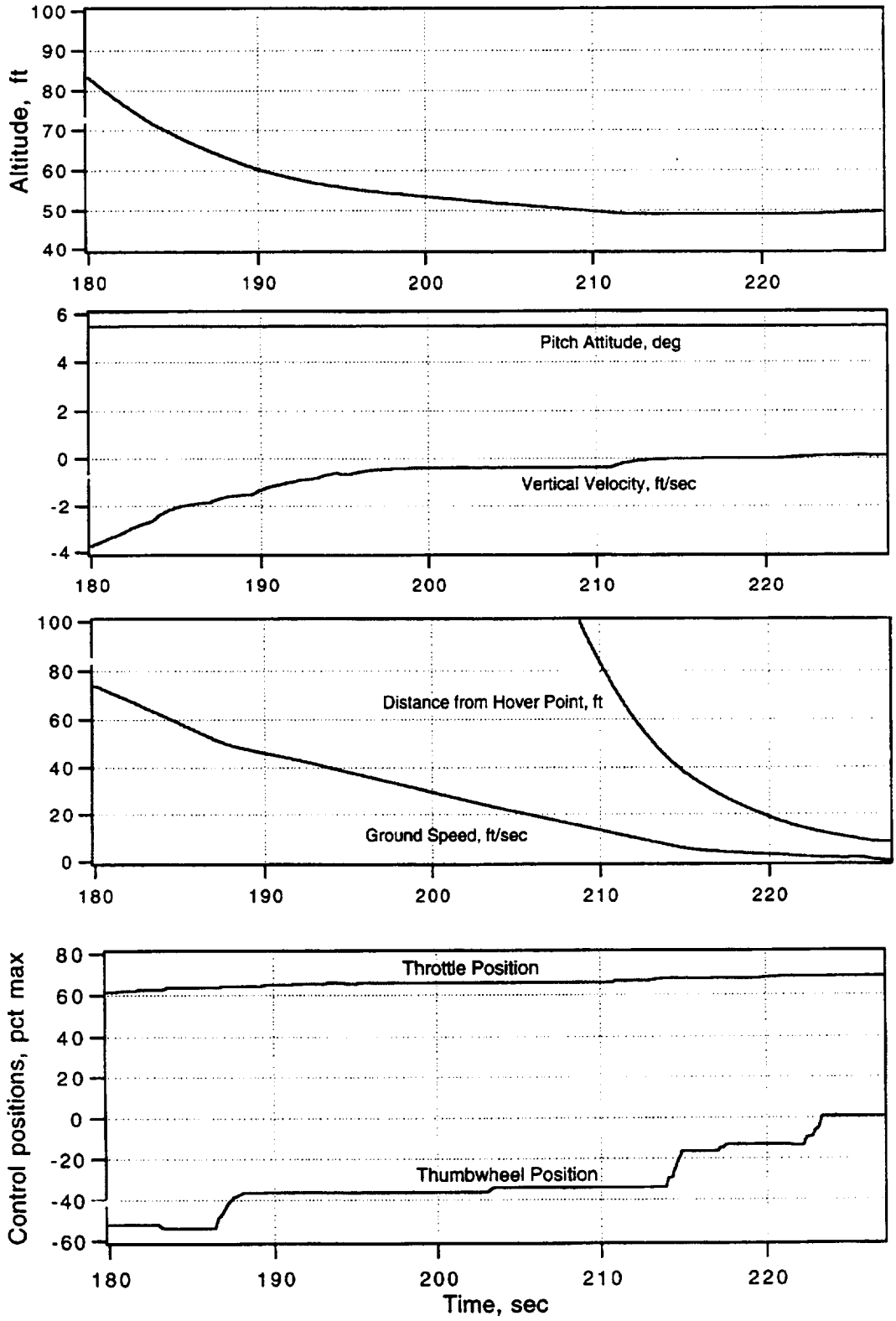

Figure 13. Time history of hover point acquisition in calm air.

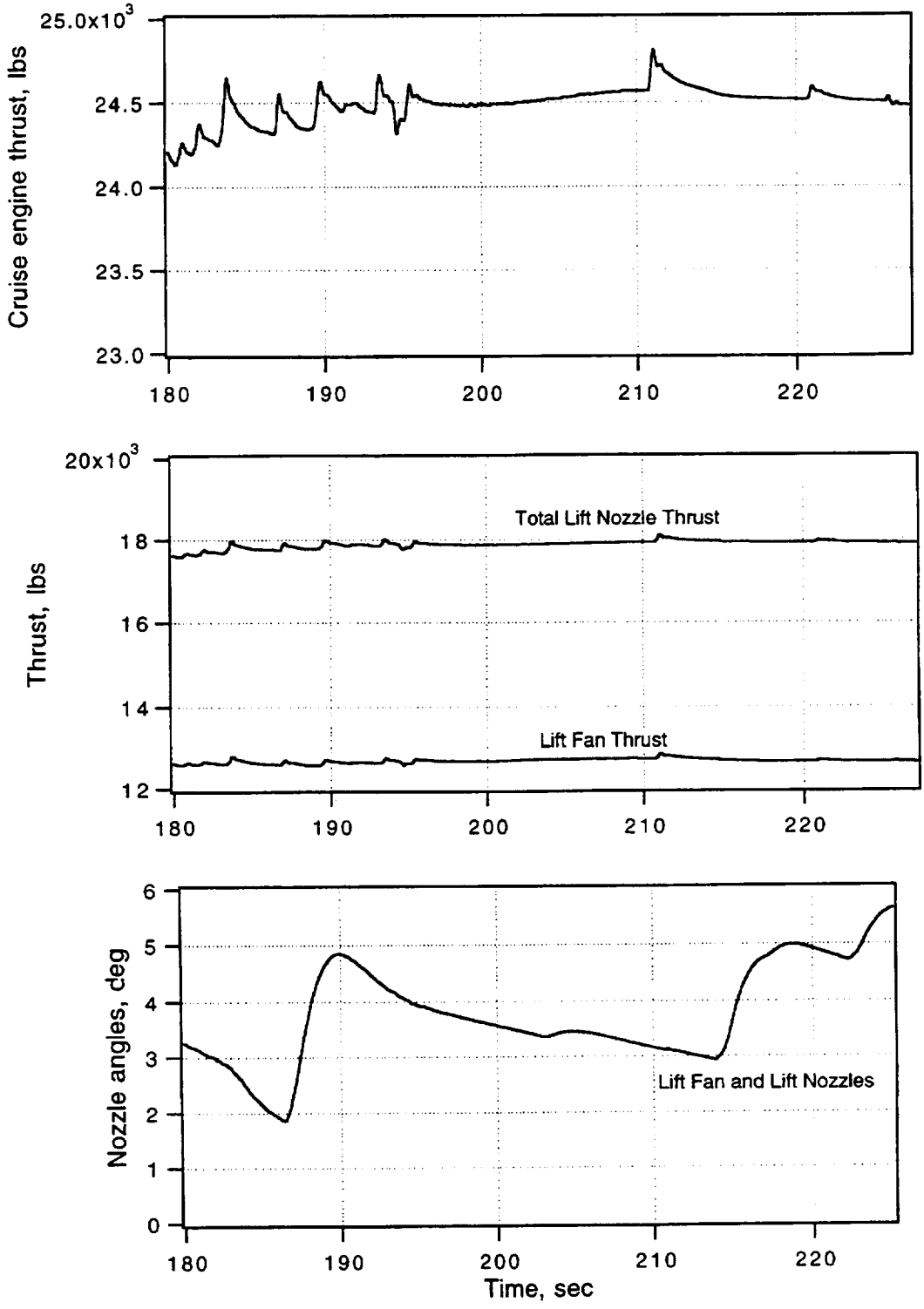

Figure 13. Concluded.

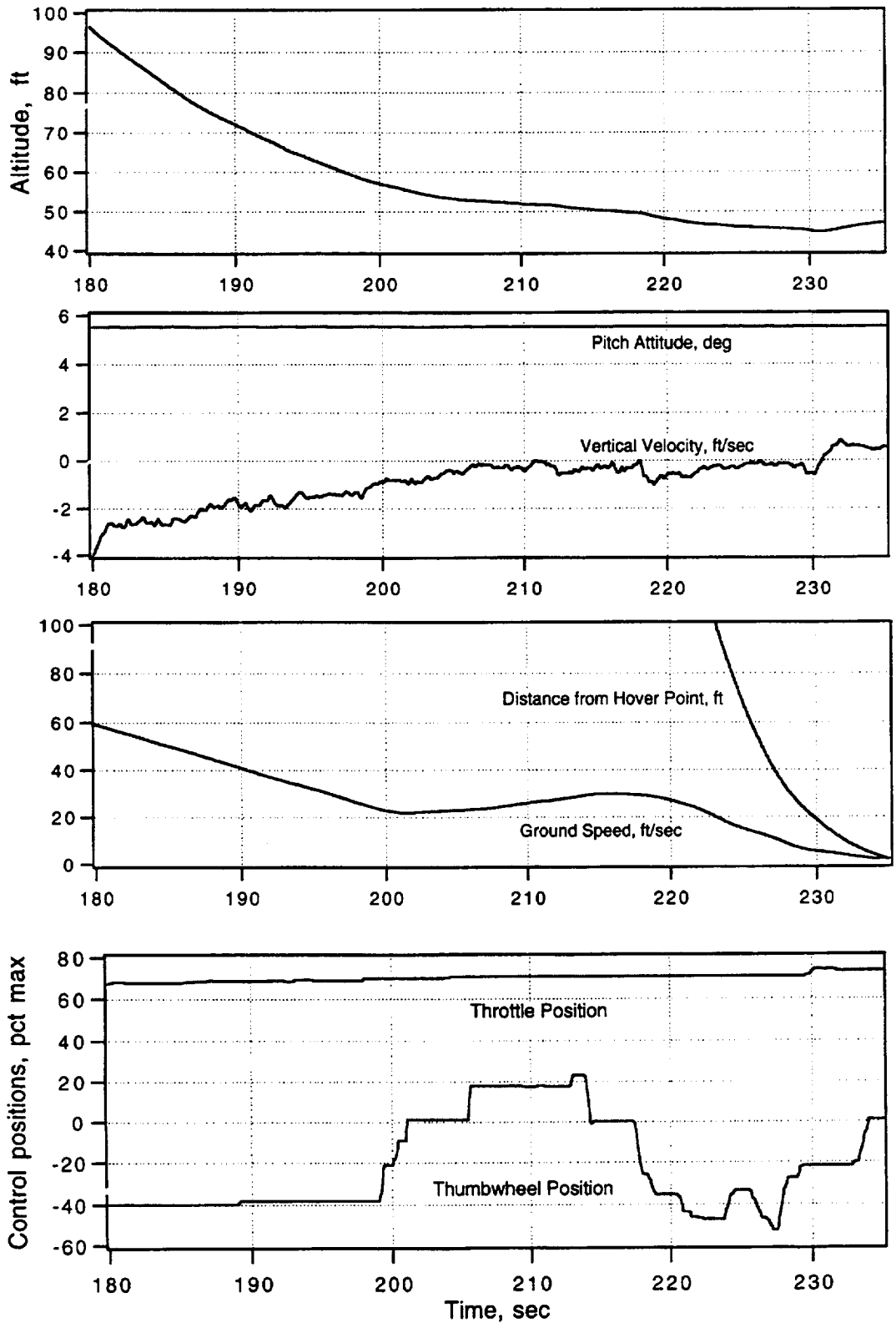

Figure 14. Time history of hover point acquisition in 6 ft/sec rms turbulence.

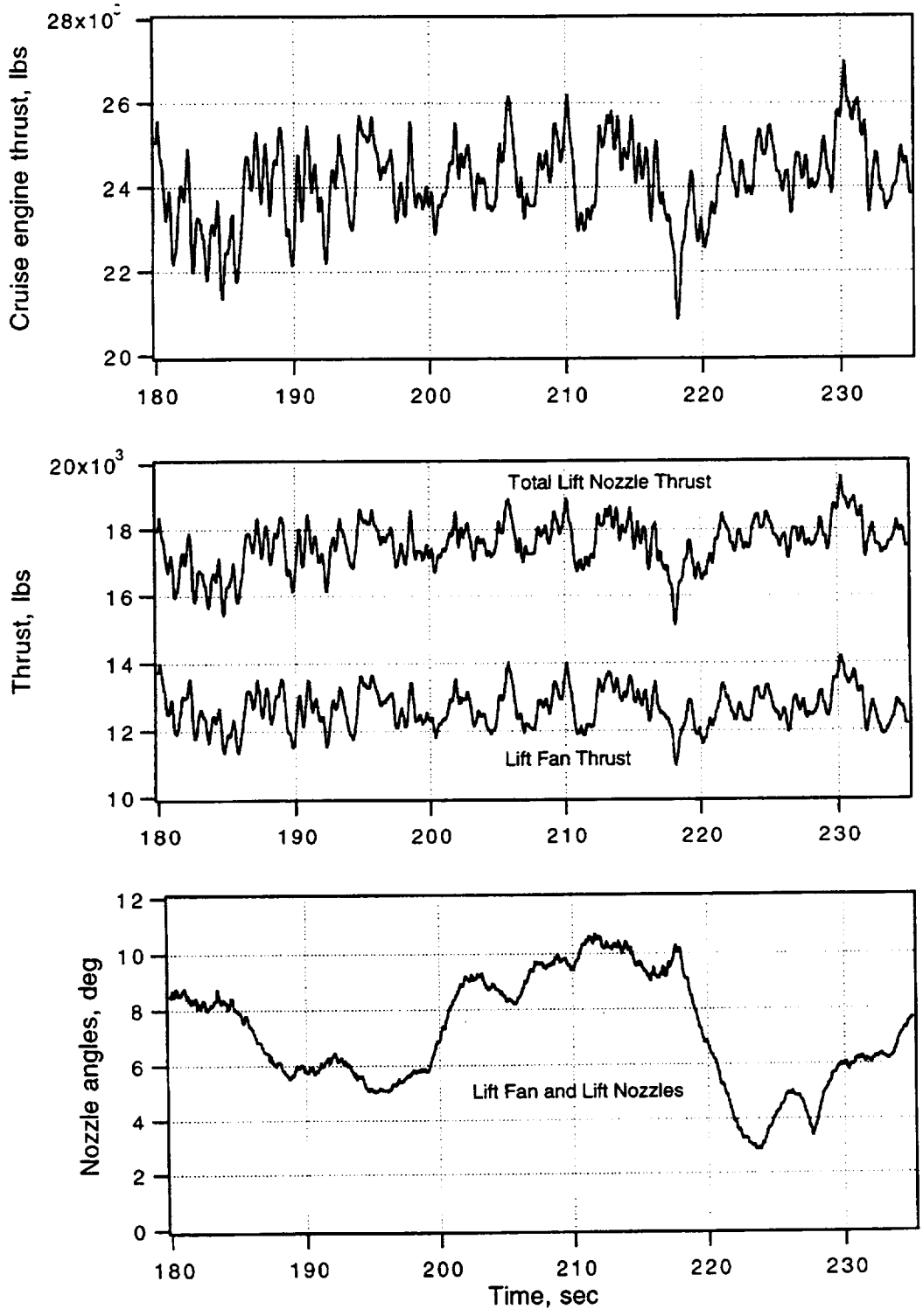

Figure 14. Concluded.

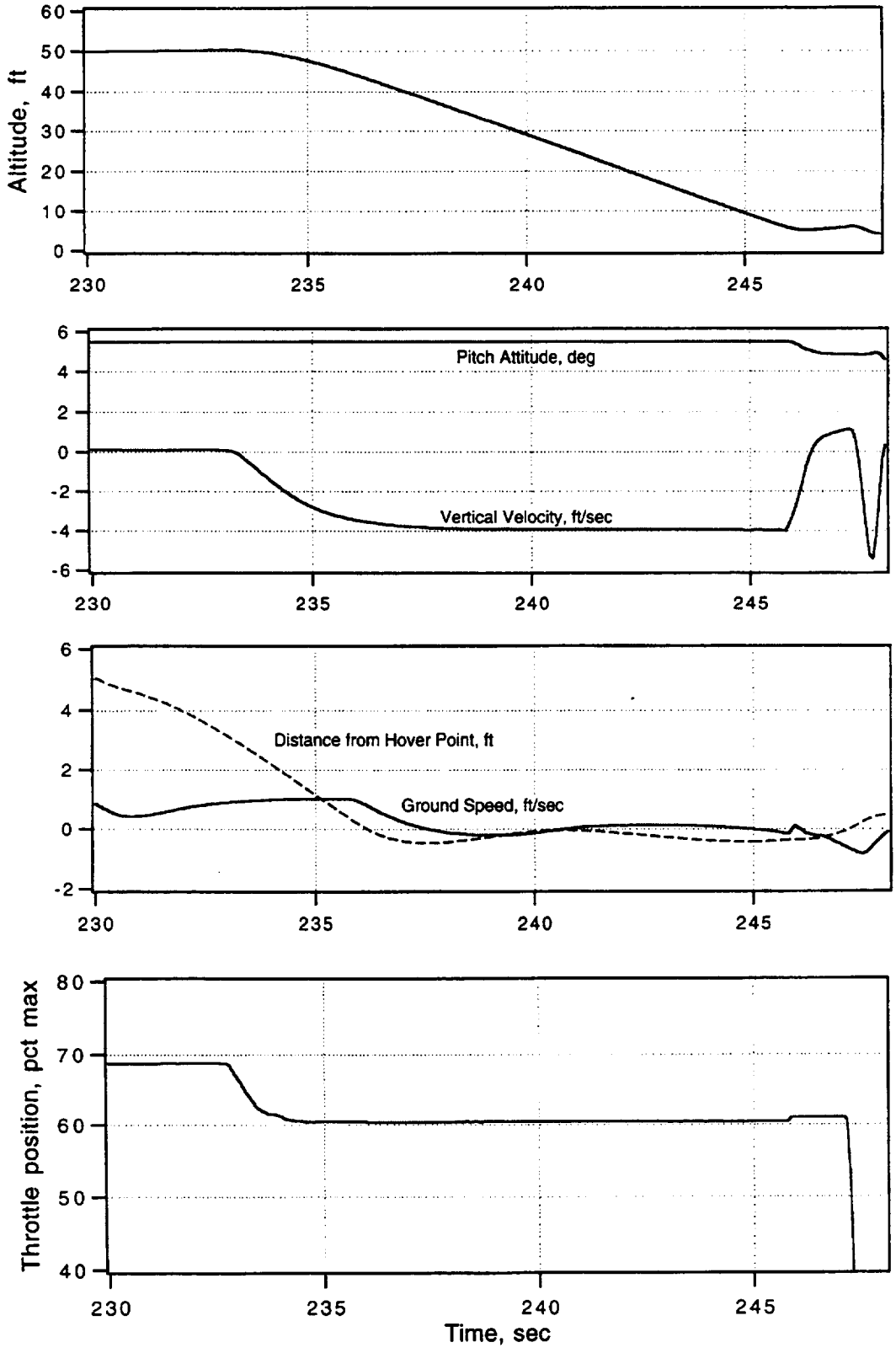

Figure 15. Time history of vertical landing in calm air.

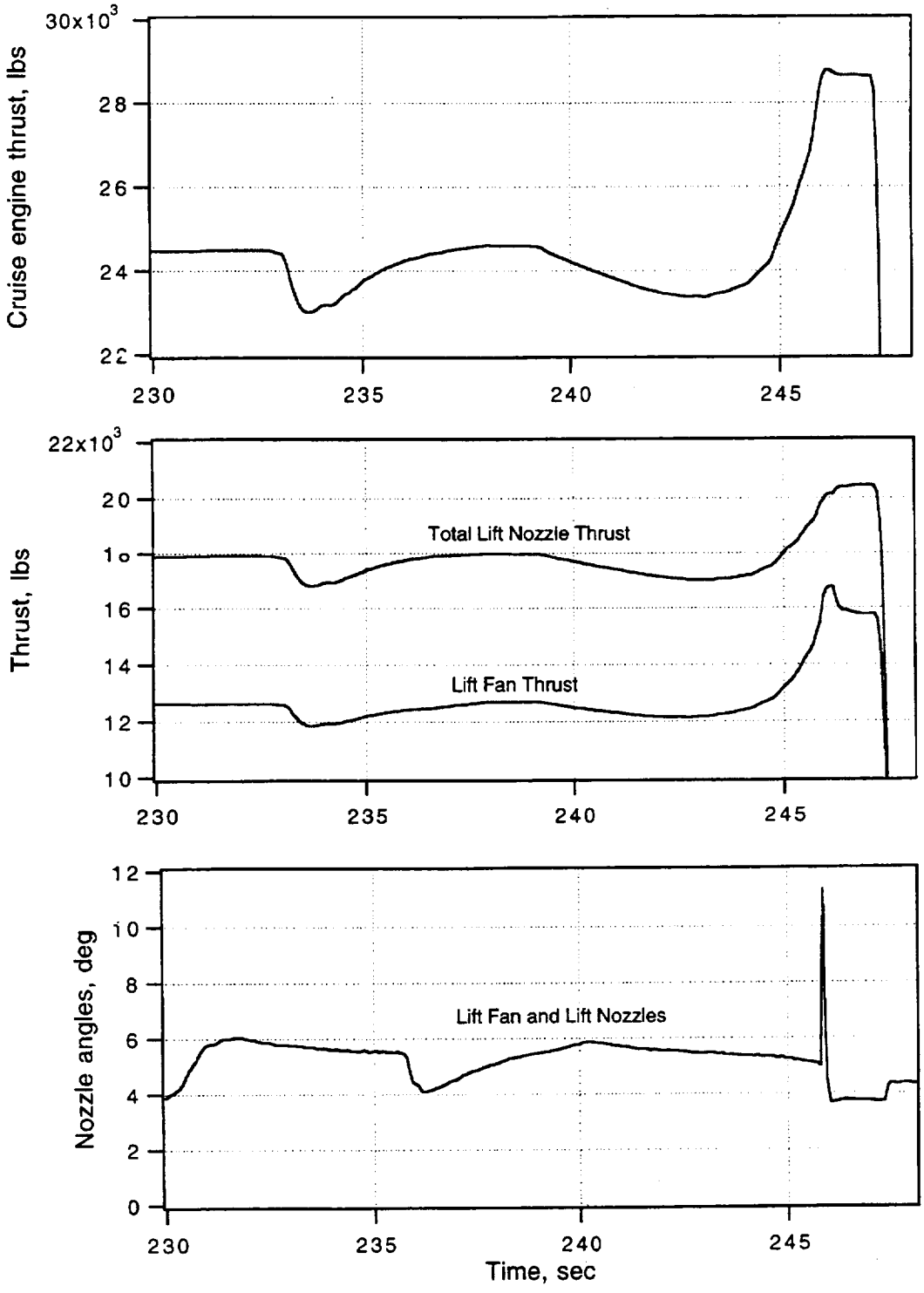

Figure 15. Concluded.

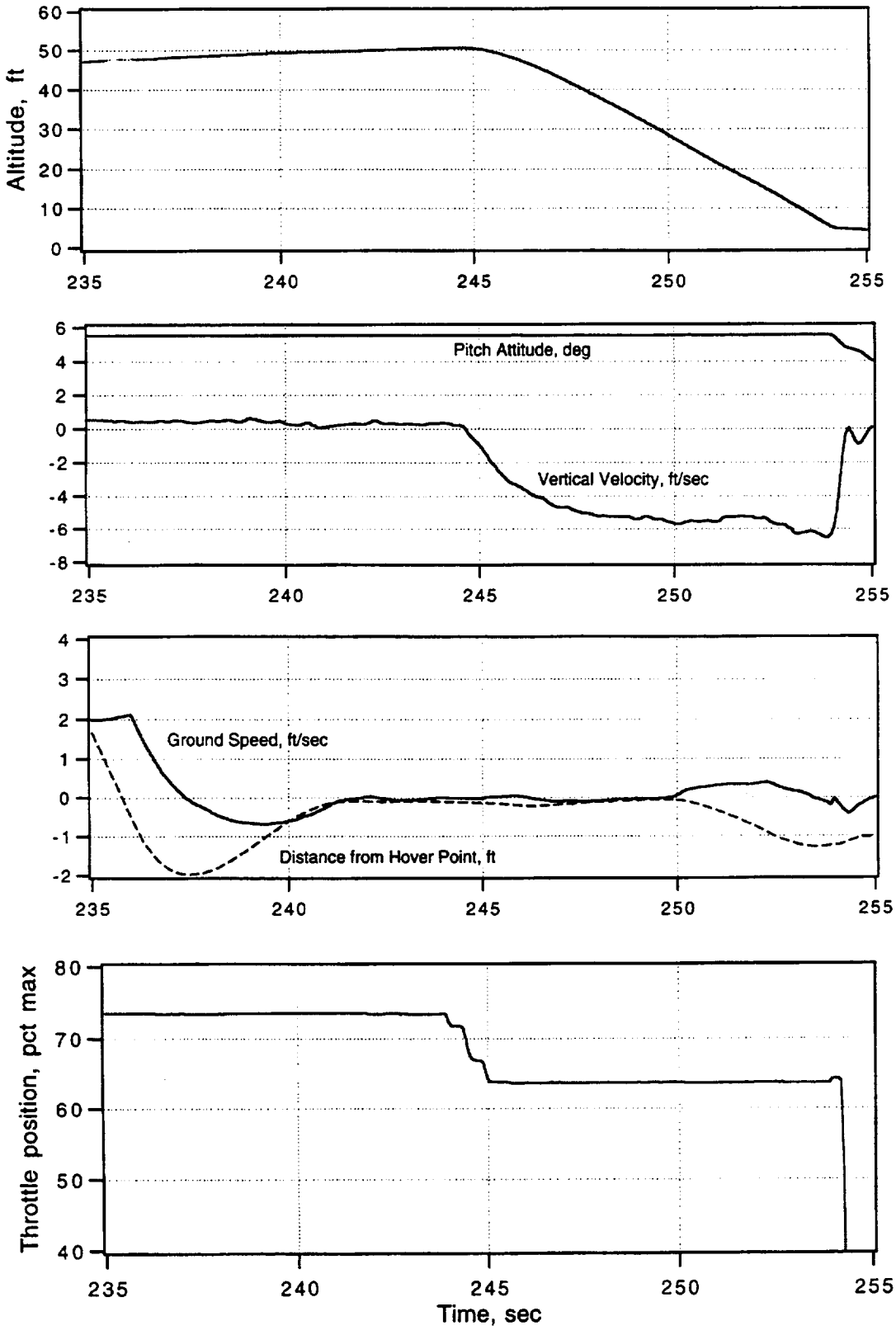

Figure 16. Time history of vertical landing in 6 ft/sec rms turbulence.

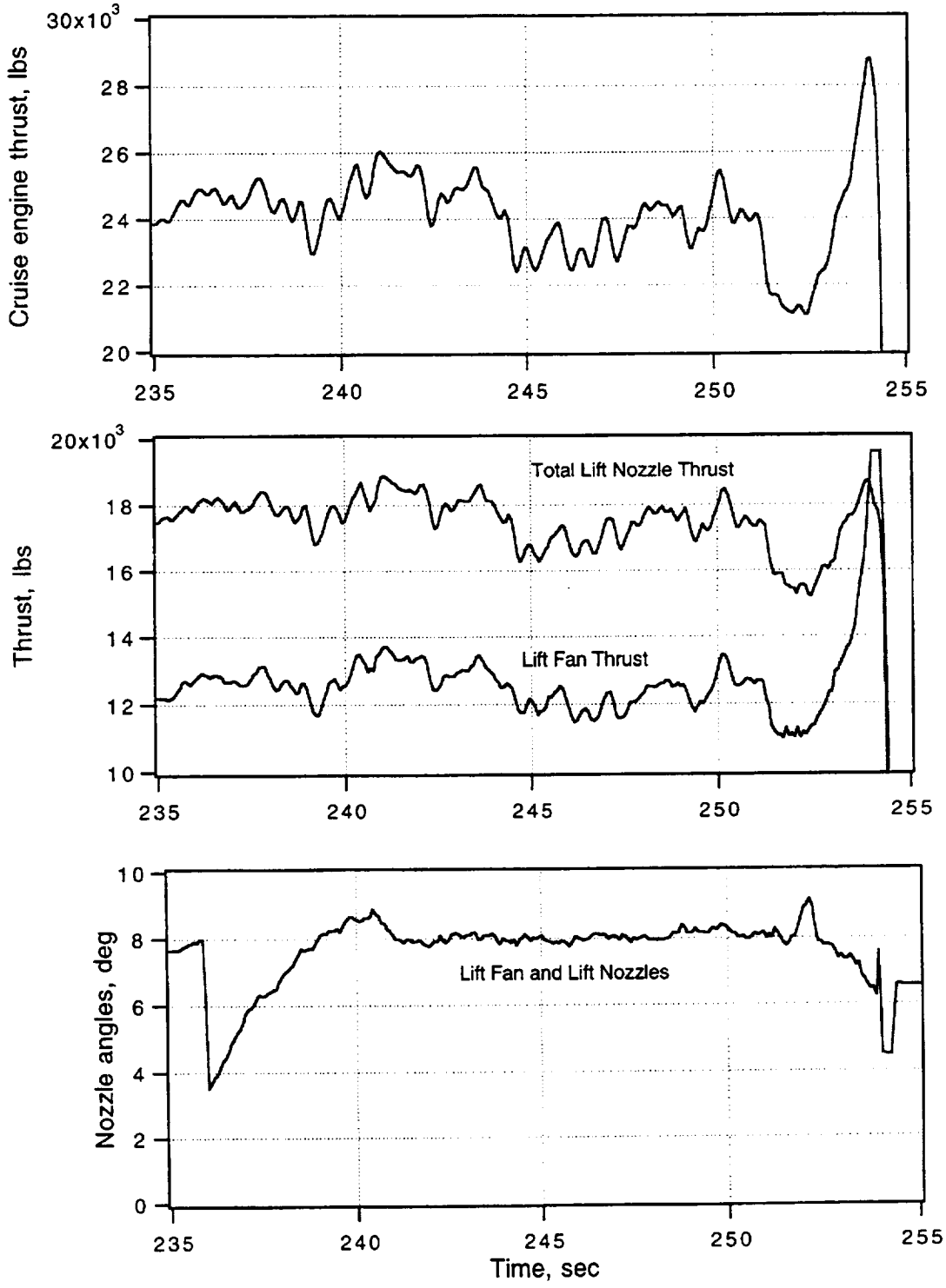

Figure 16. Concluded.

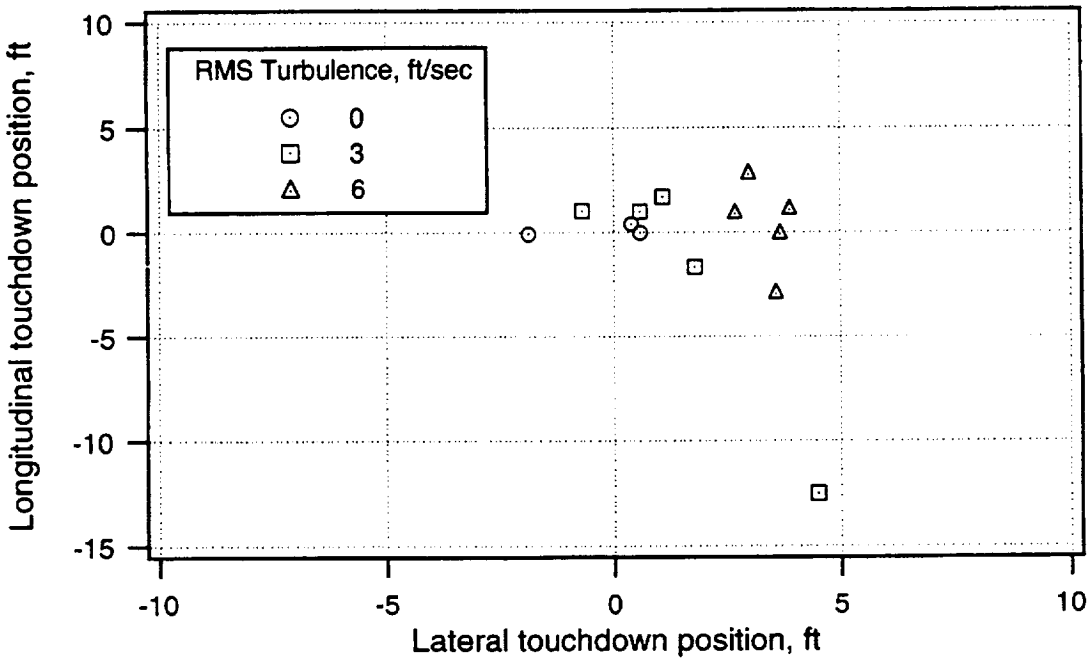

(a) Runway landing

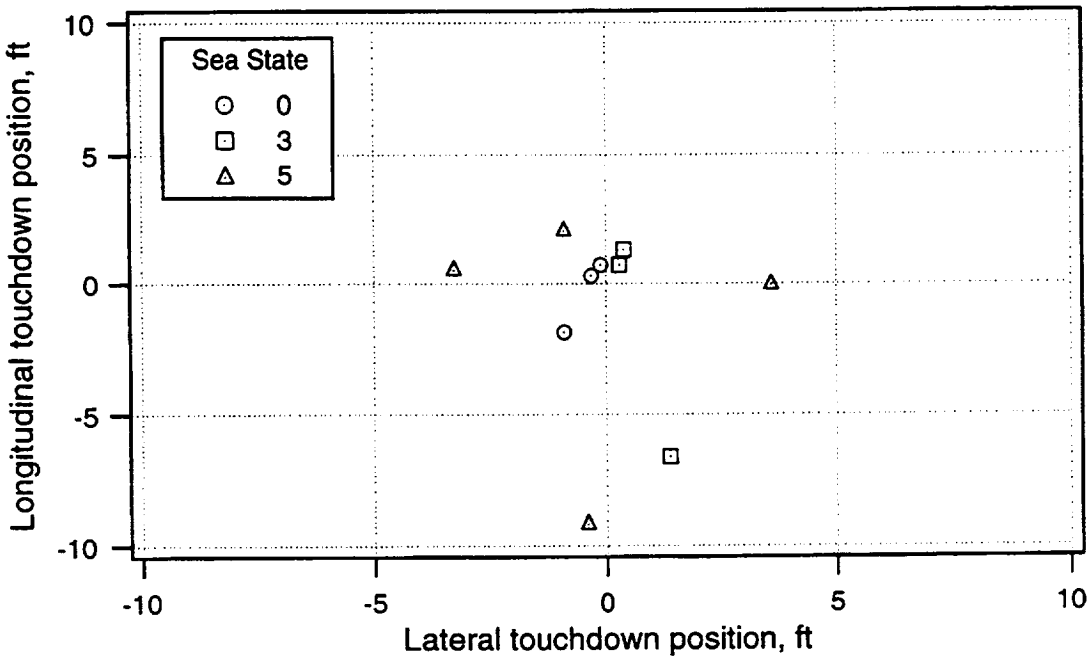

(b) Shipboard landing

Figure 17. Touchdown position accuracy for runway and shipboard landings.

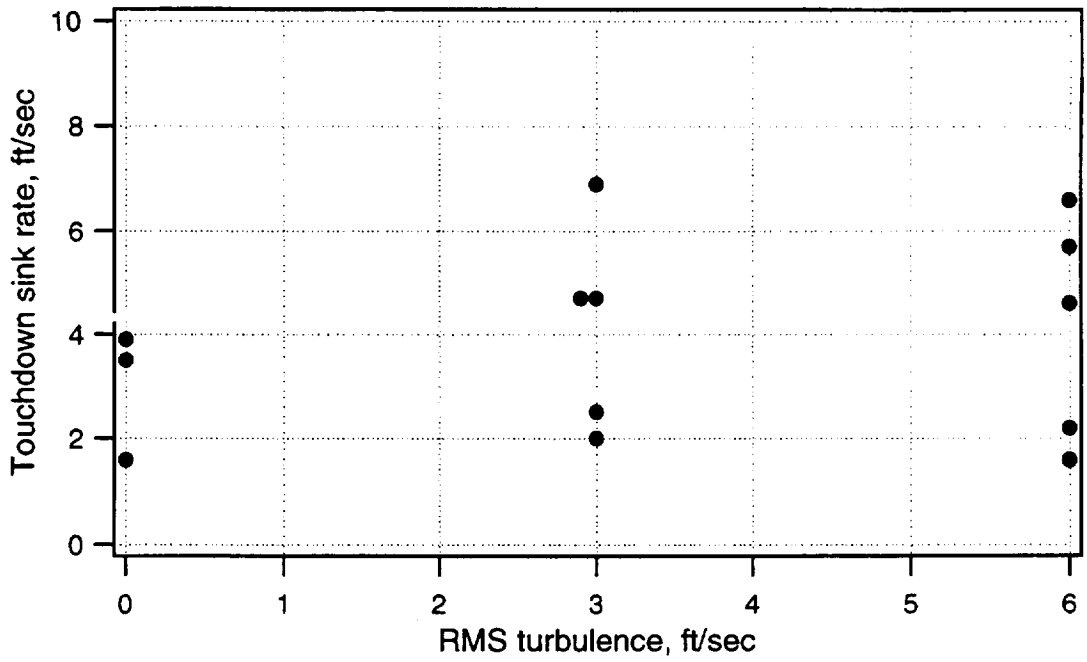

(a) Runway landing

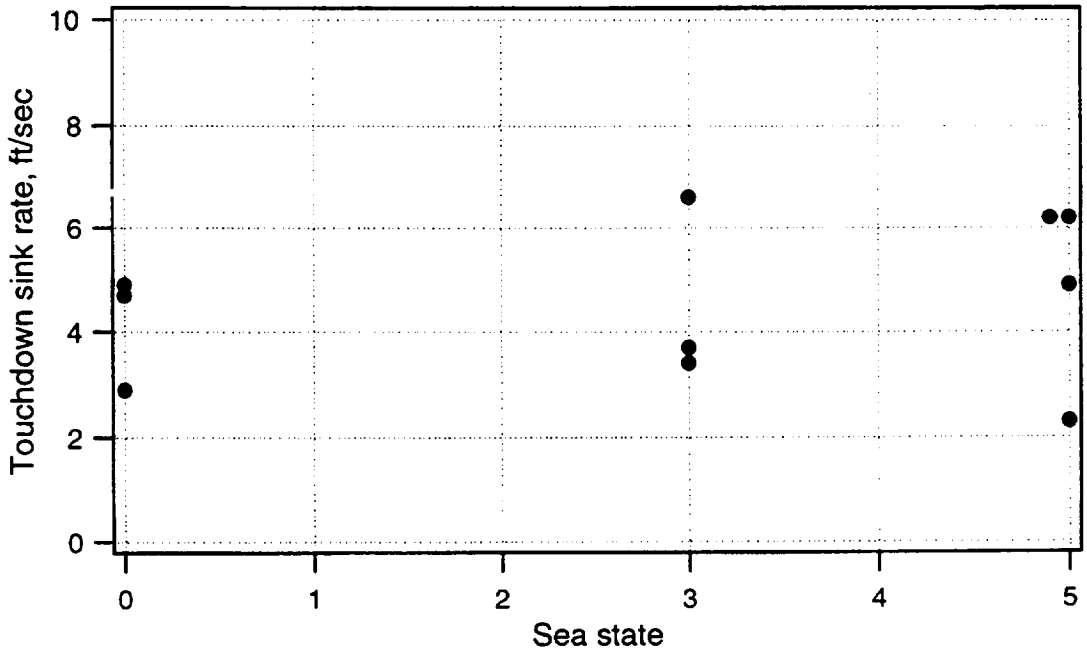

(b) Shipboard landing

Figure 18. Touchdown sink rate for runway and shipboard landings.

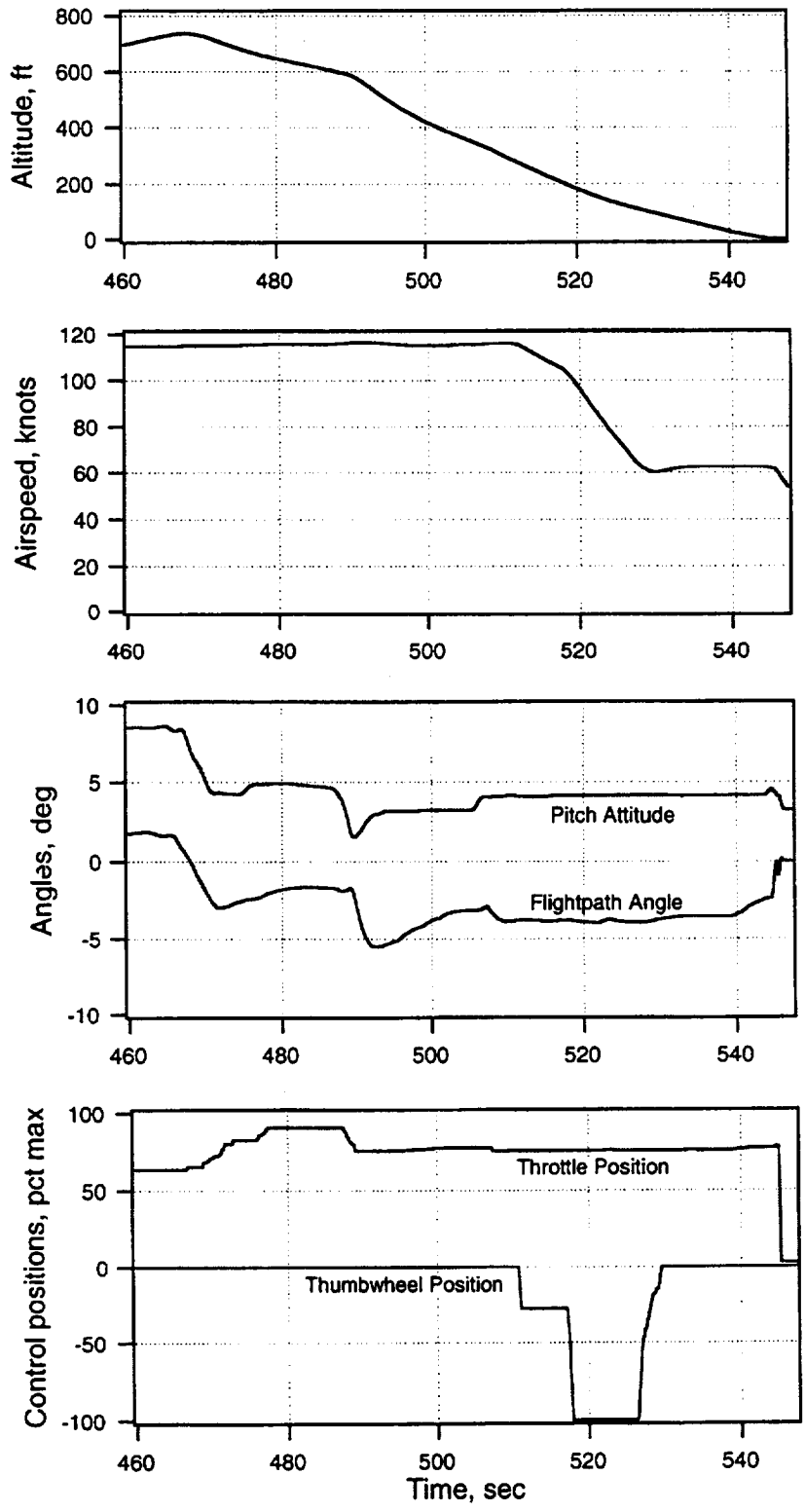

Figure 19. Time history of decelerating transition to slow landing.

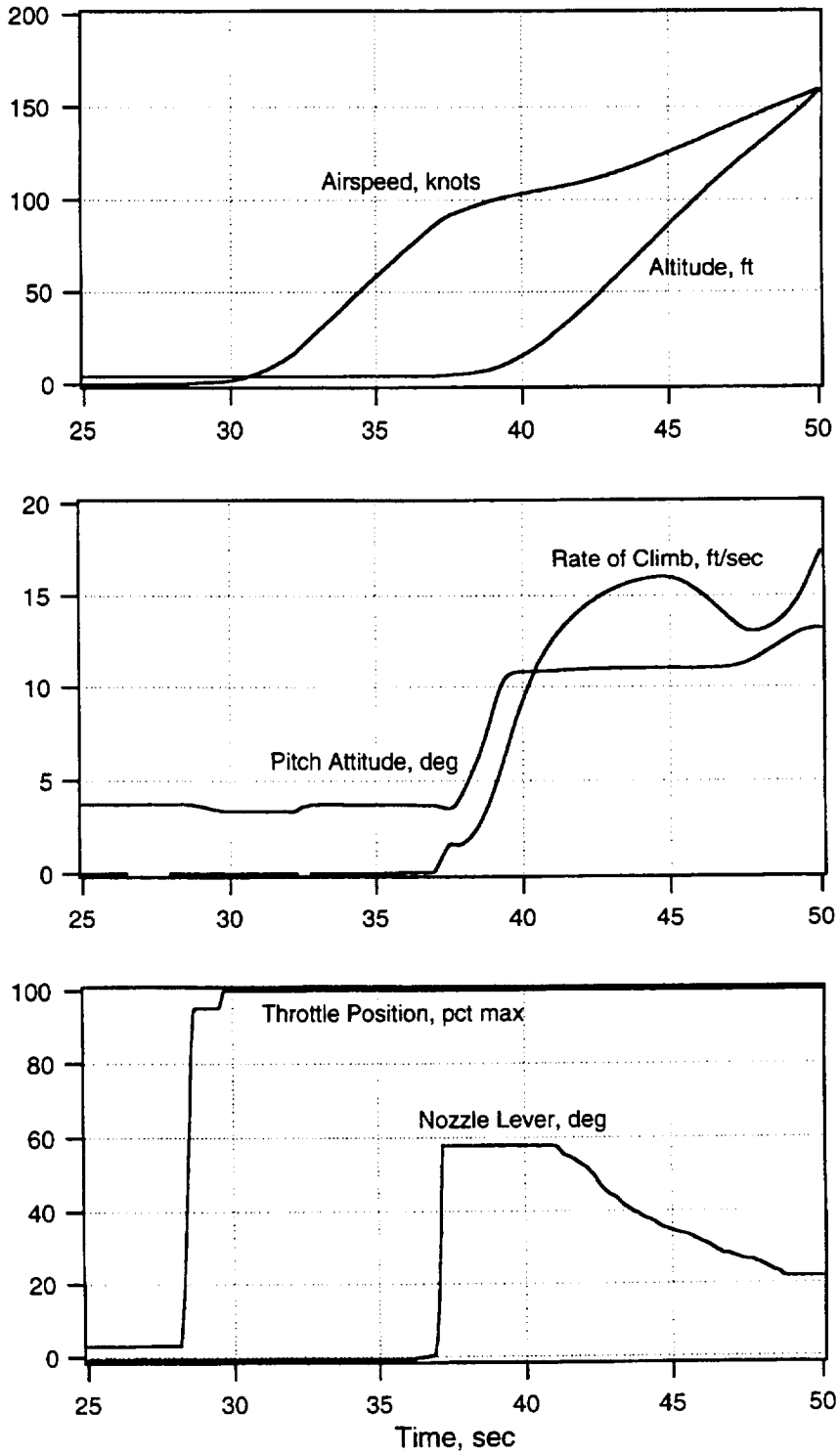

Figure 20. Time history of a short takeoff from runway at 40,000 gross weight.

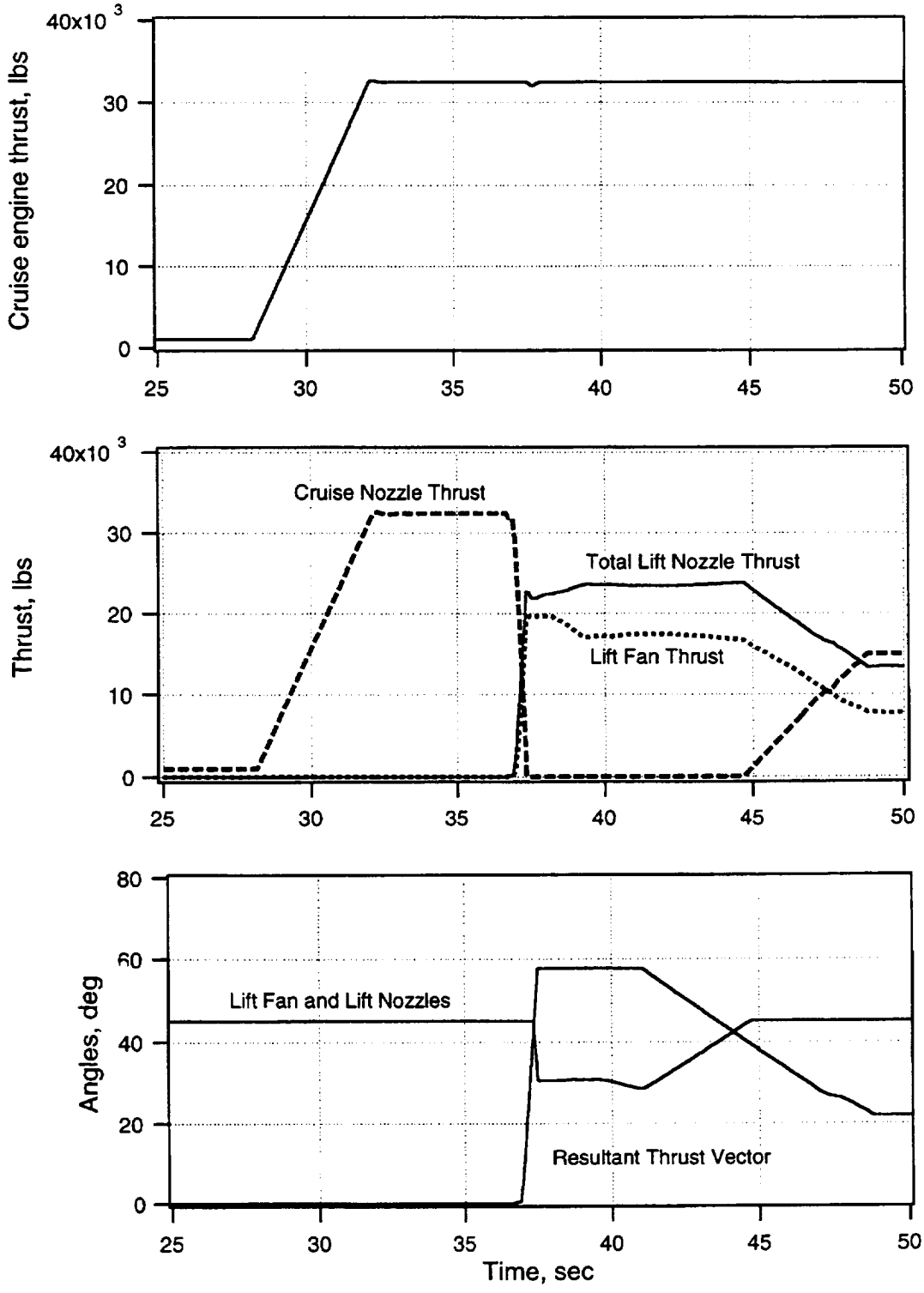

Figure 20. Concluded.

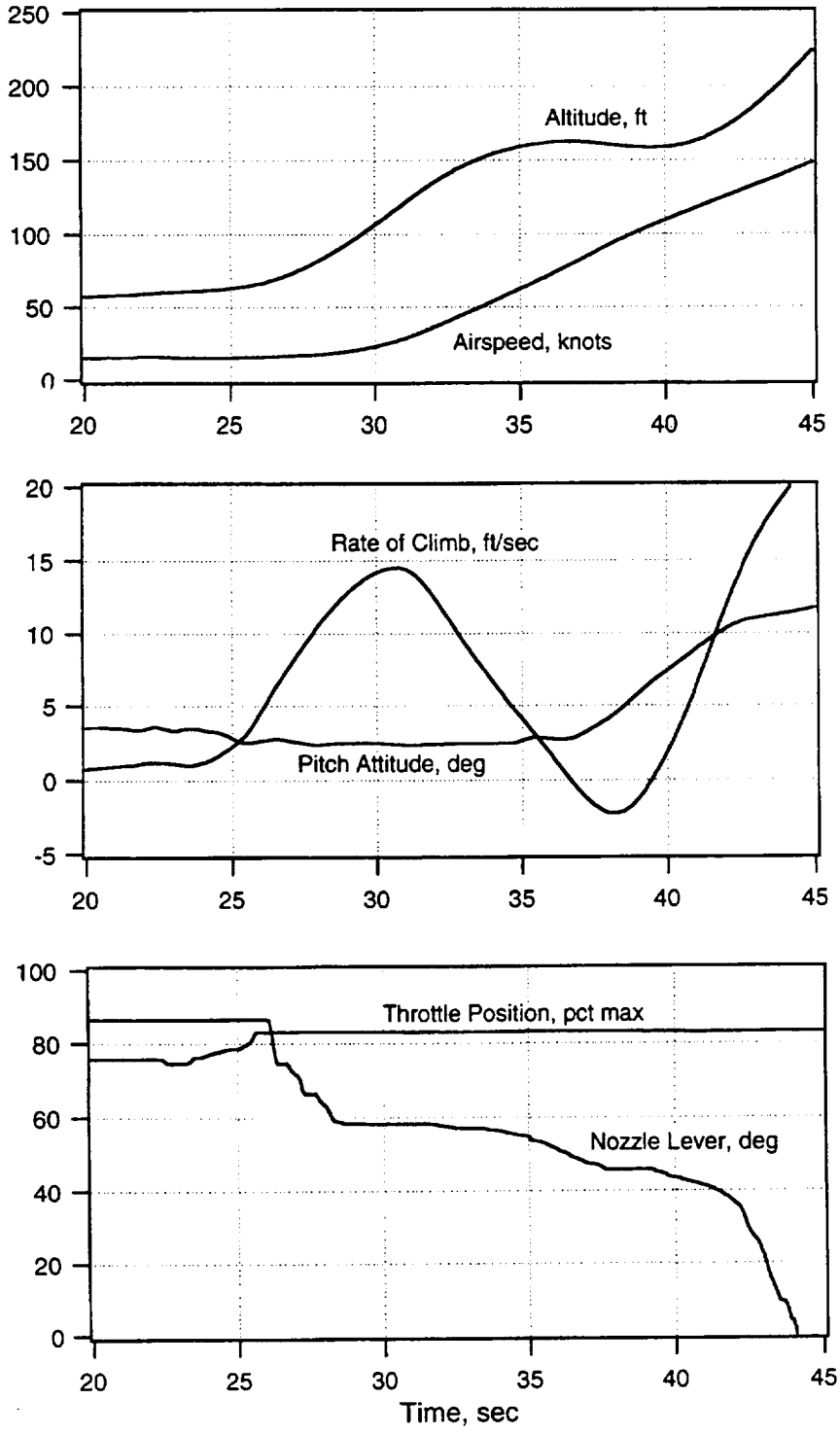

Figure 21. Time history of acceleration from hover to wing-borne flight.

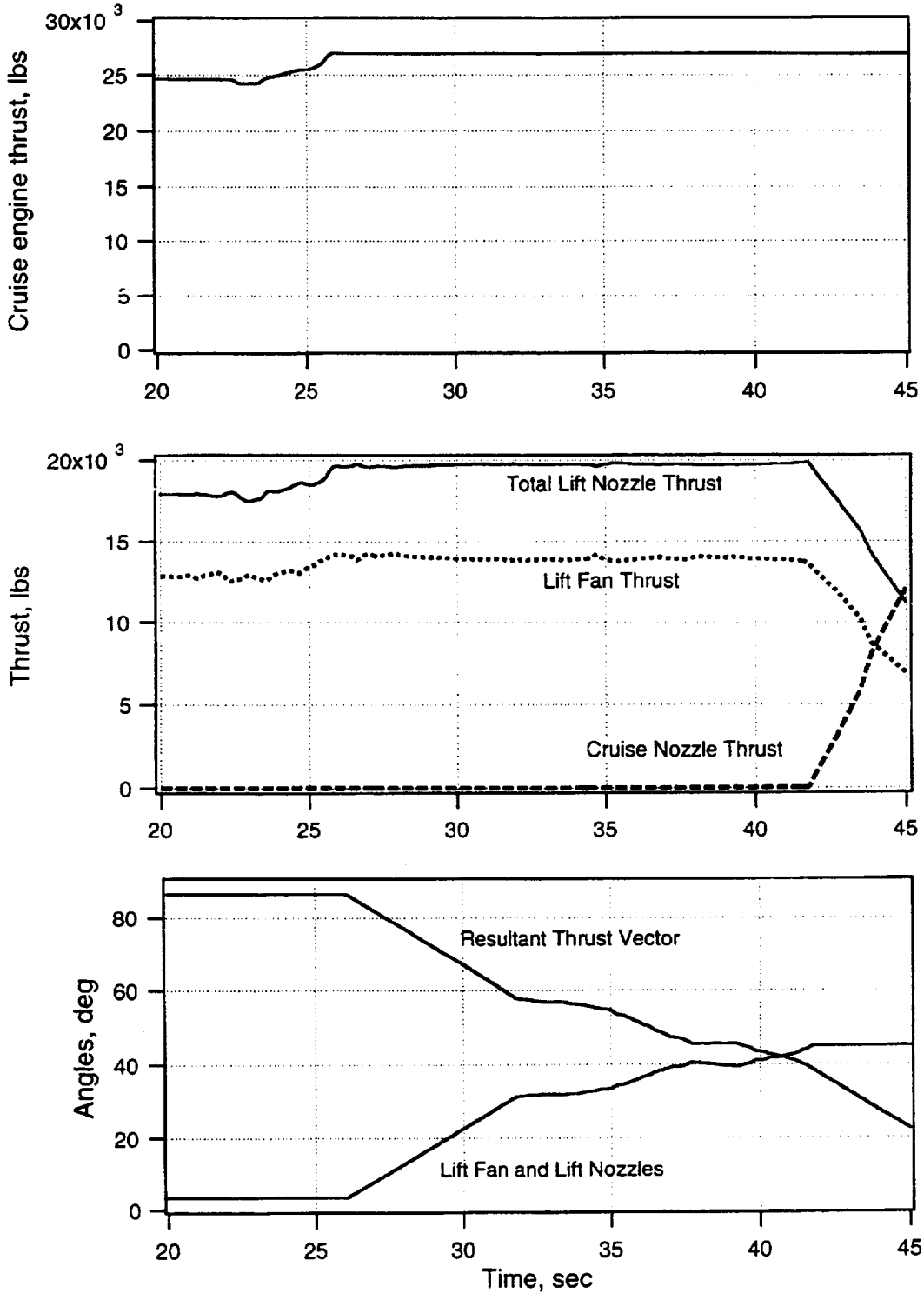

Figure 21. Concluded.

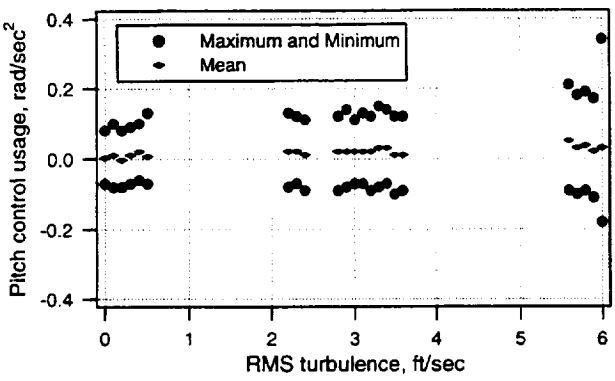

(a) Decelerating approach

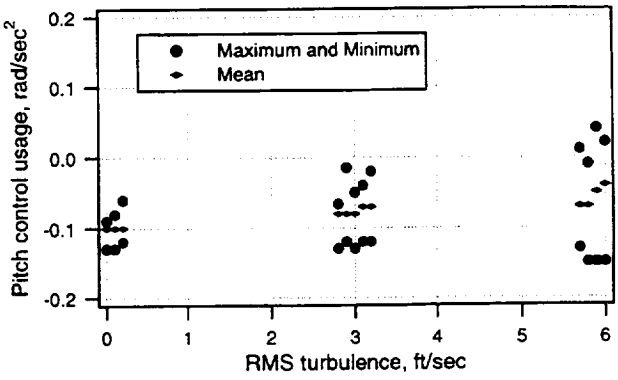

(c) Runway landing

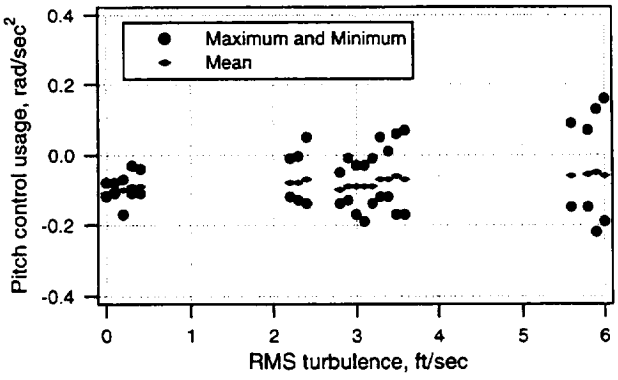

(b) Hover point acquisition

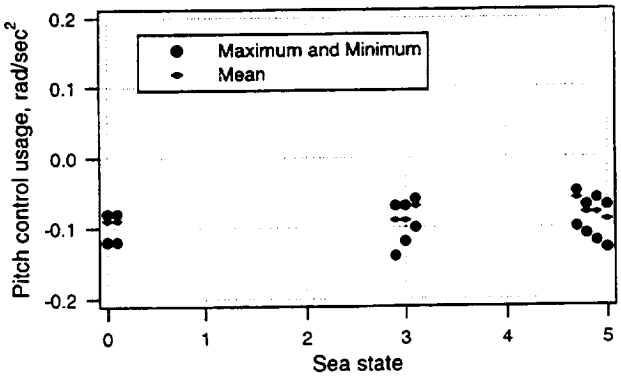

(d) Shipboard landing

Figure 22. Pitch control usage for approach and landing tasks.

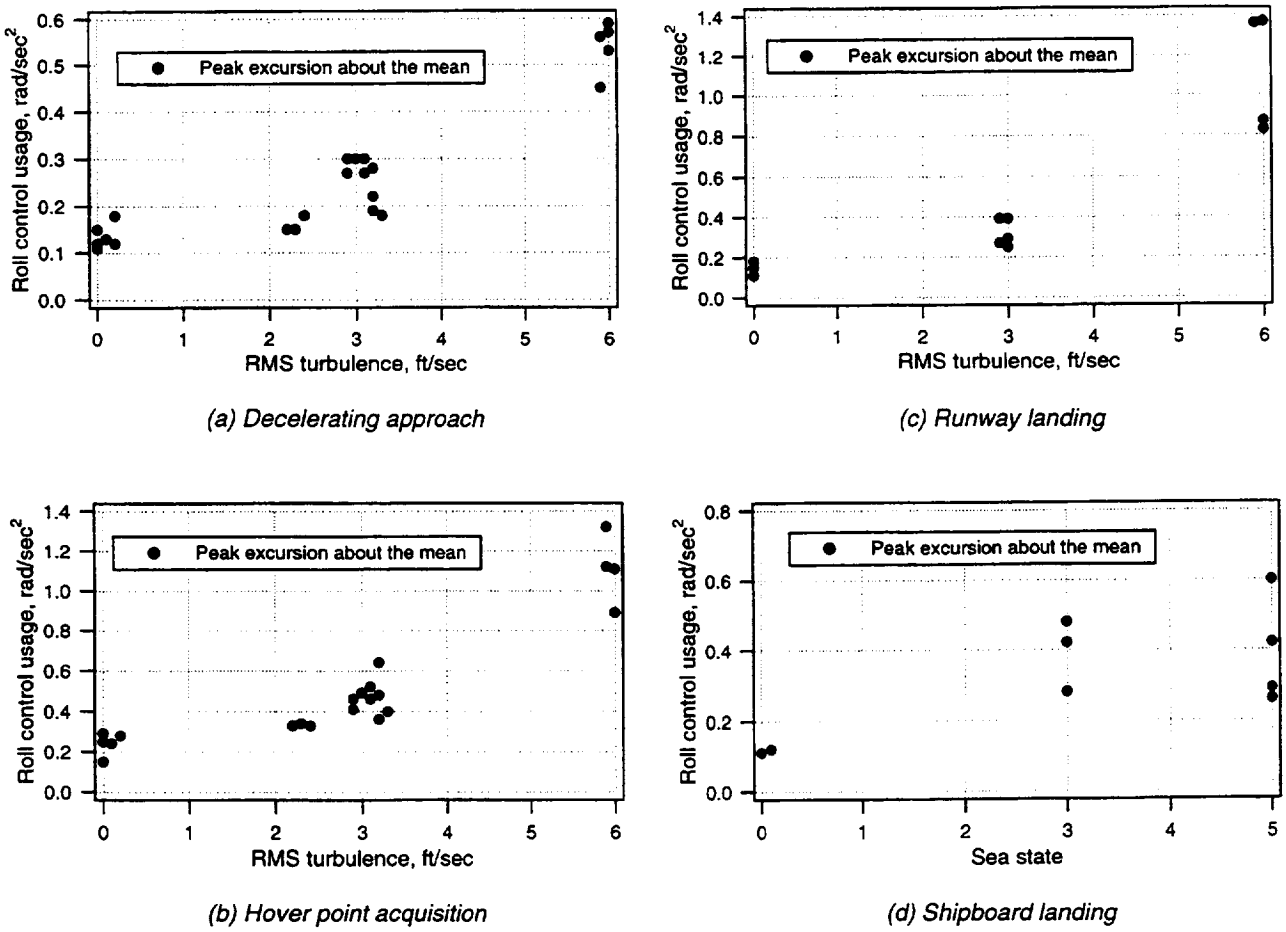

Figure 23. Roll control usage for approach and landing tasks.

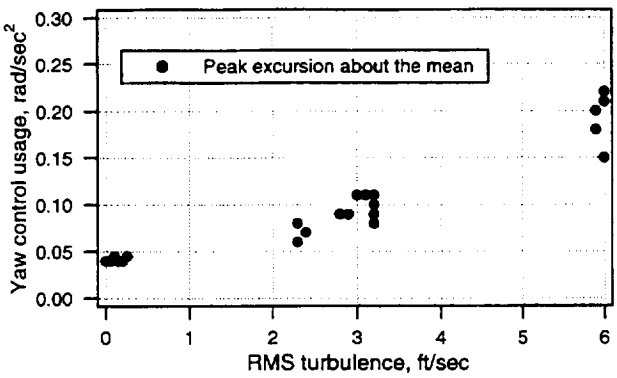

(a) Decelerating approach

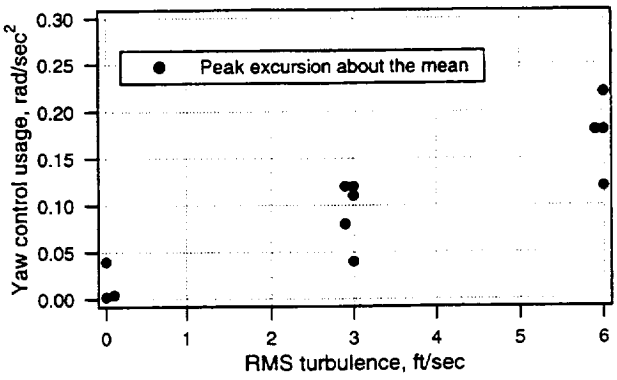

(c) Runway landing

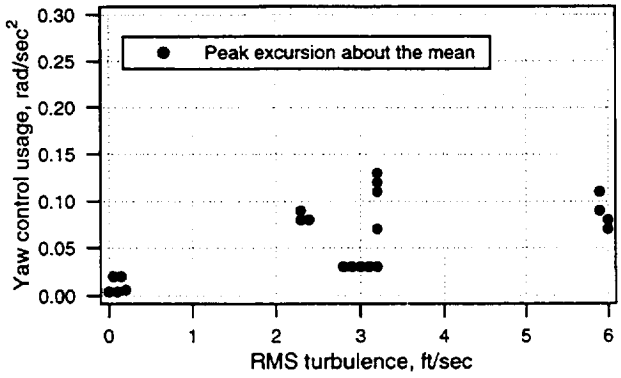

(b) Hover point acquisition

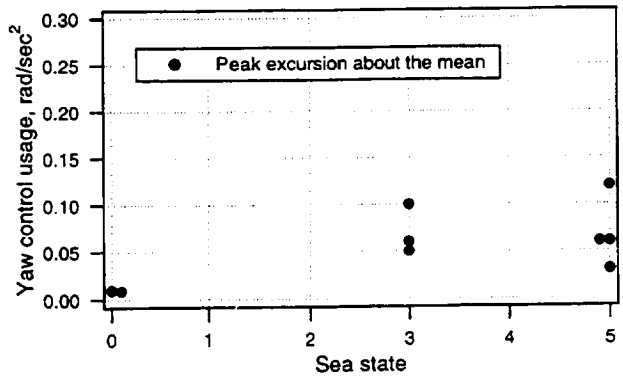

(d) Shipboard landing

Figure 24. Yaw control usage for approach and landing tasks.

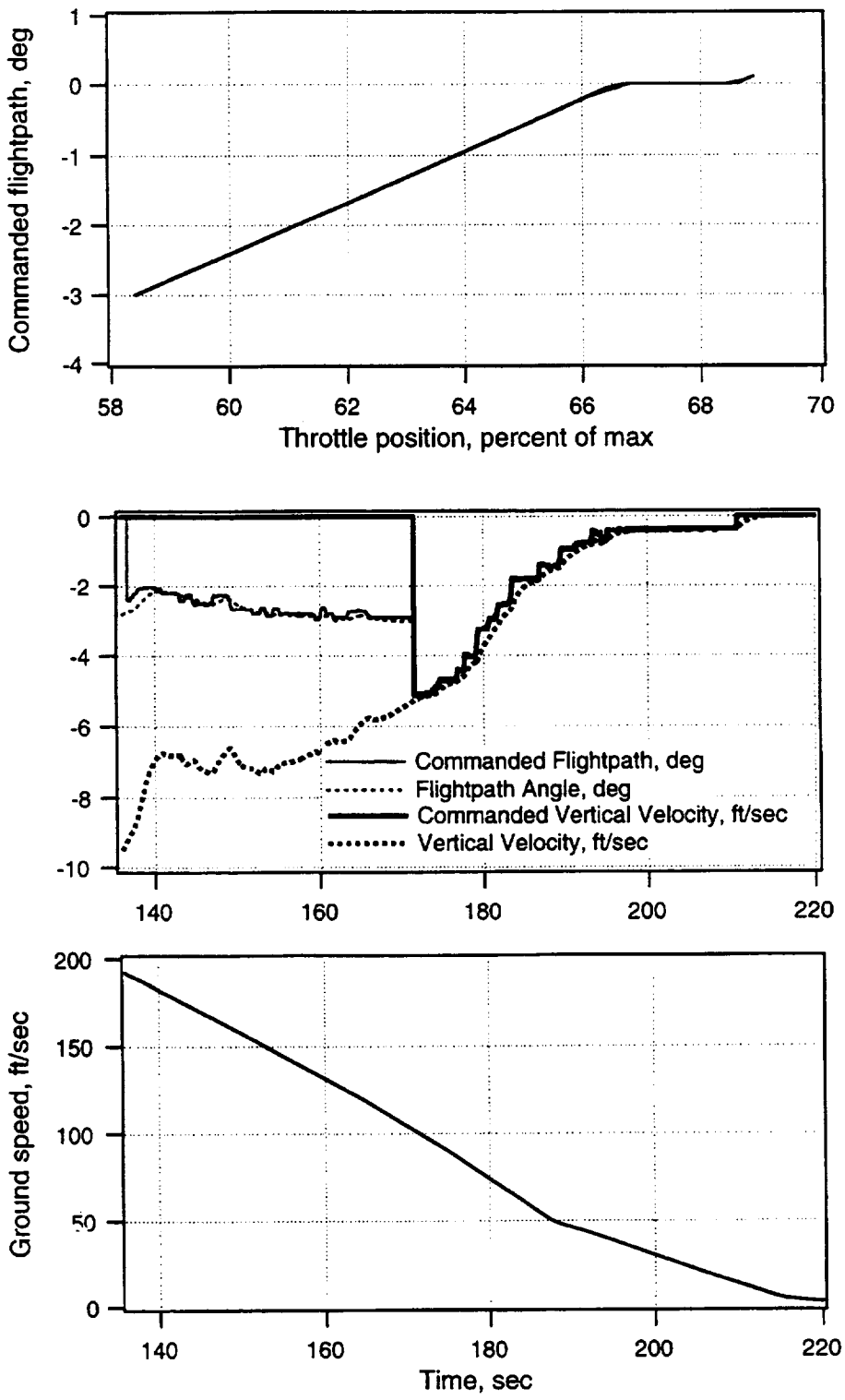

Figure 25. Characteristics of flightpath control with the throttle.

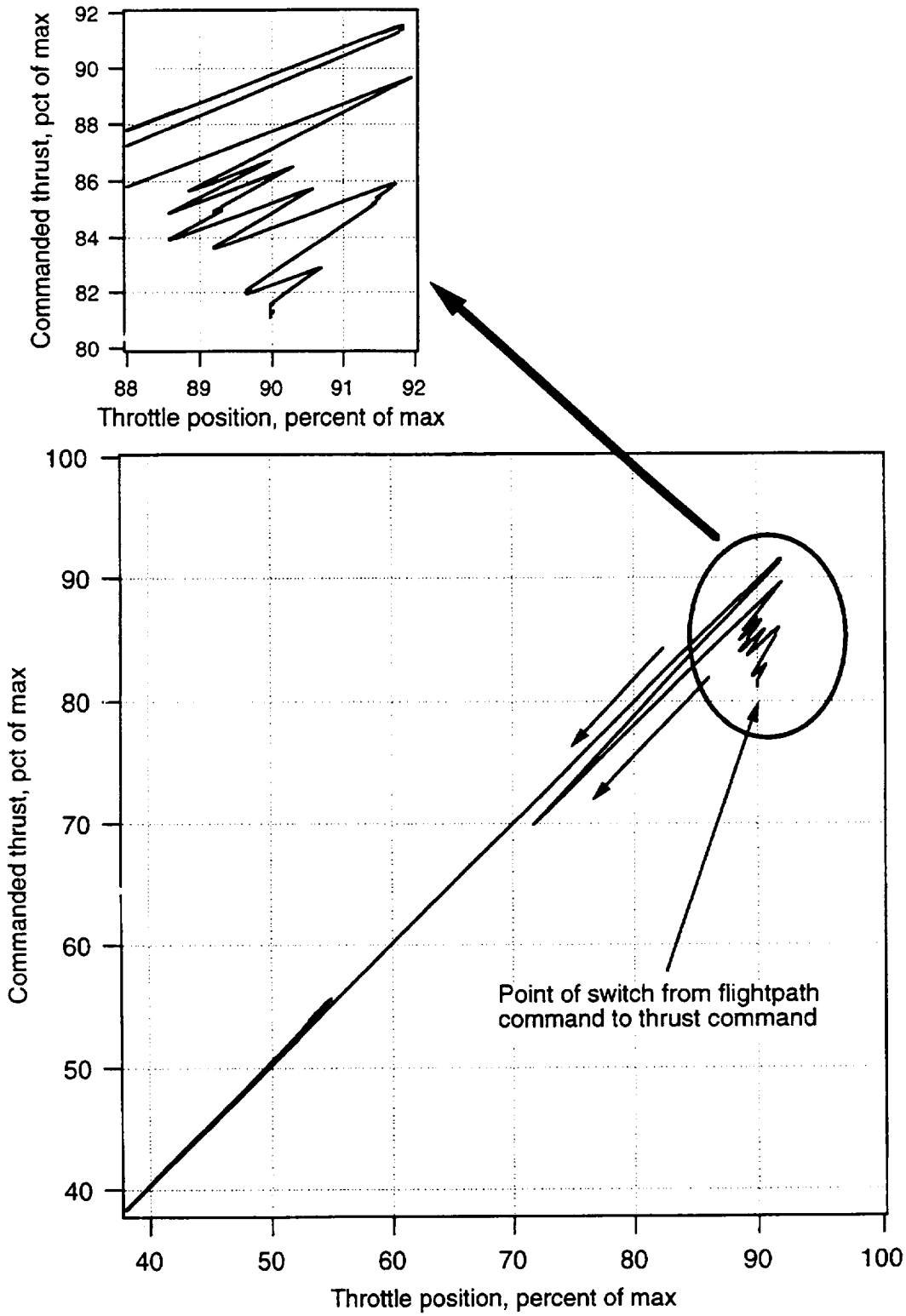

Figure 26(a). Characteristics of thrust control with the throttle.

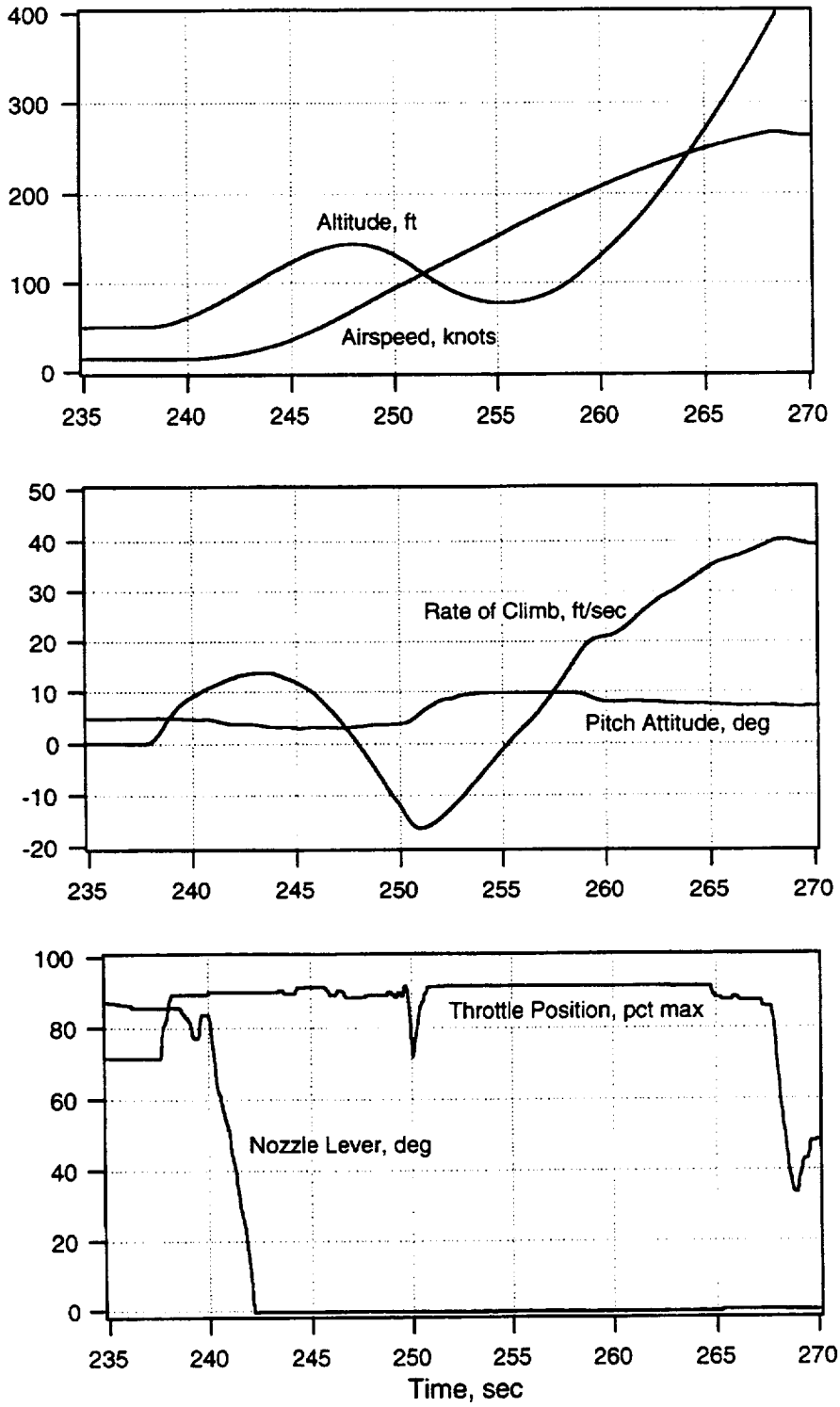

Figure 26(b). Switch from flightpath to thrust command during waveoff.

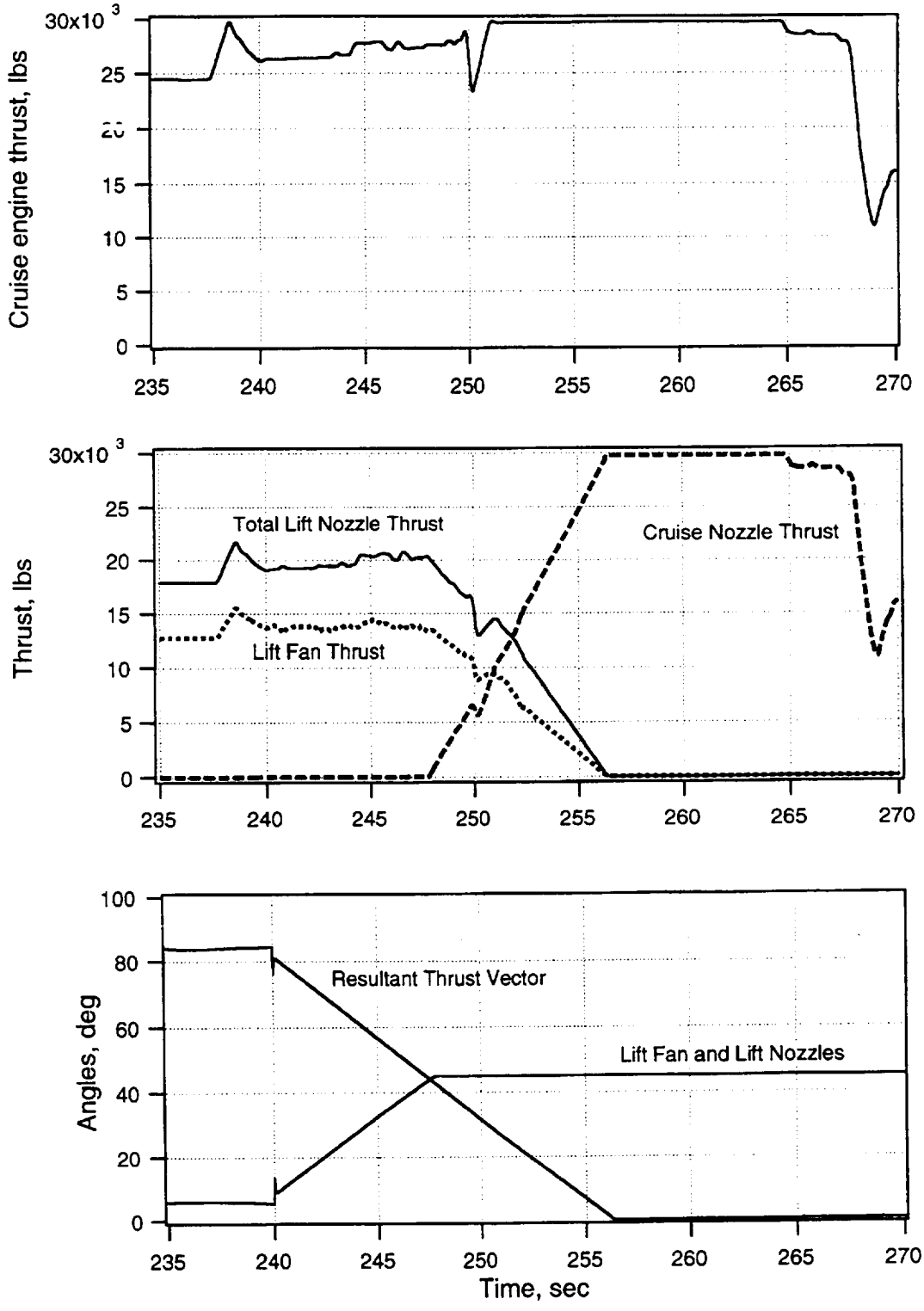

Figure 26(b). Concluded.

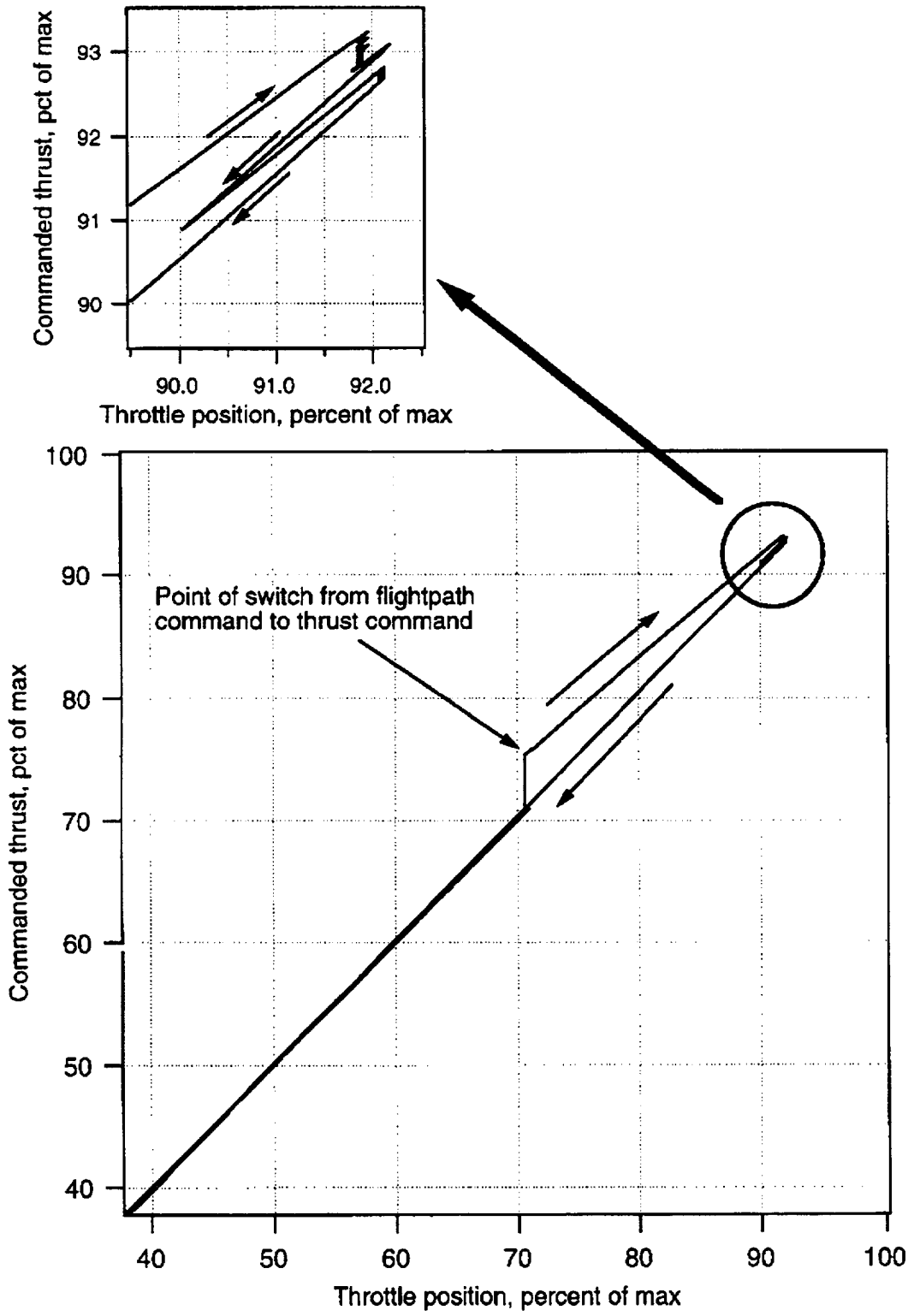

Figure 27. Characteristics of thrust control with the throttle.

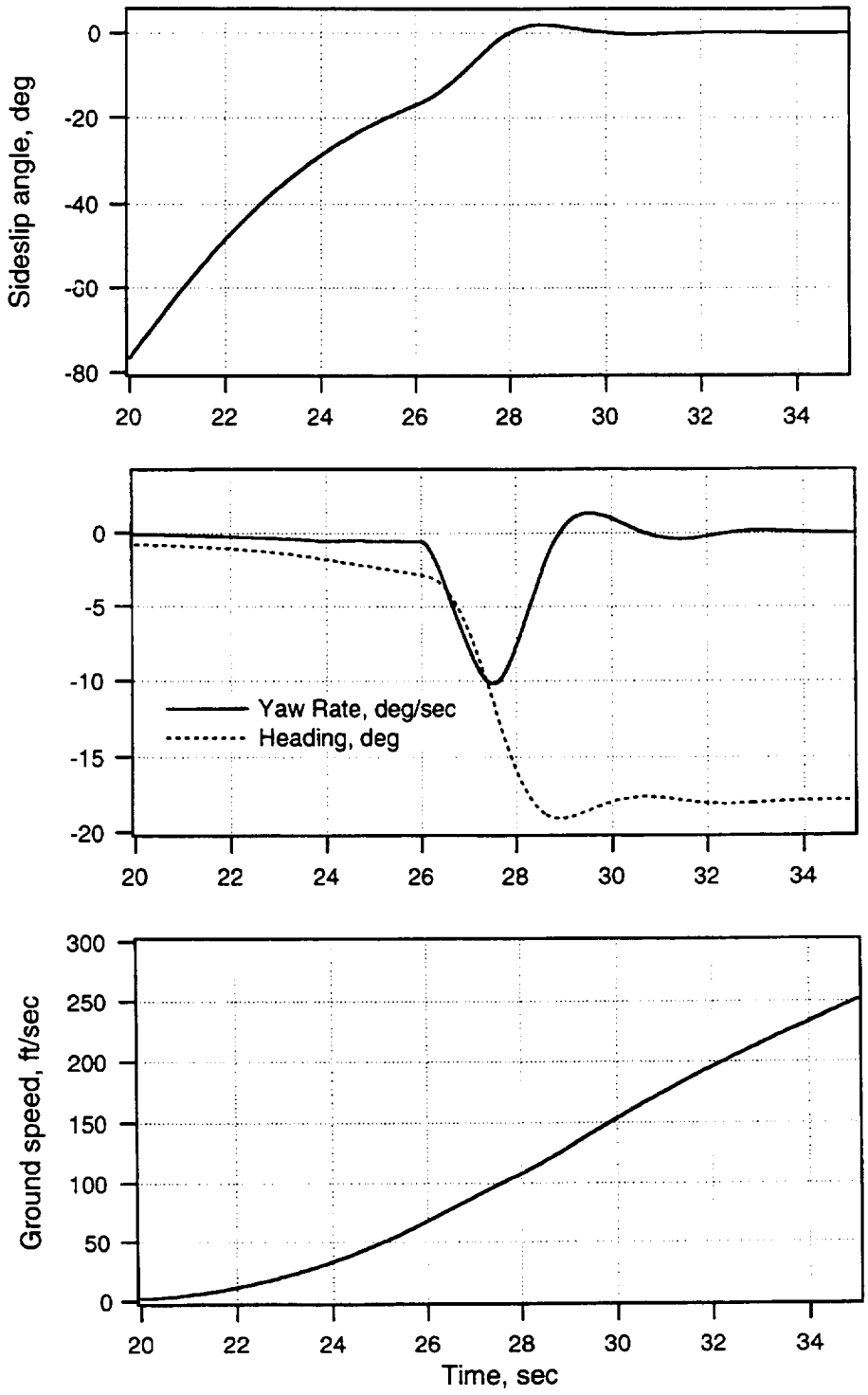

Figure 28(a). Yaw response during acceleration from hover in 15 knot crosswind for yaw mode blending range from 40 to 60 knots.

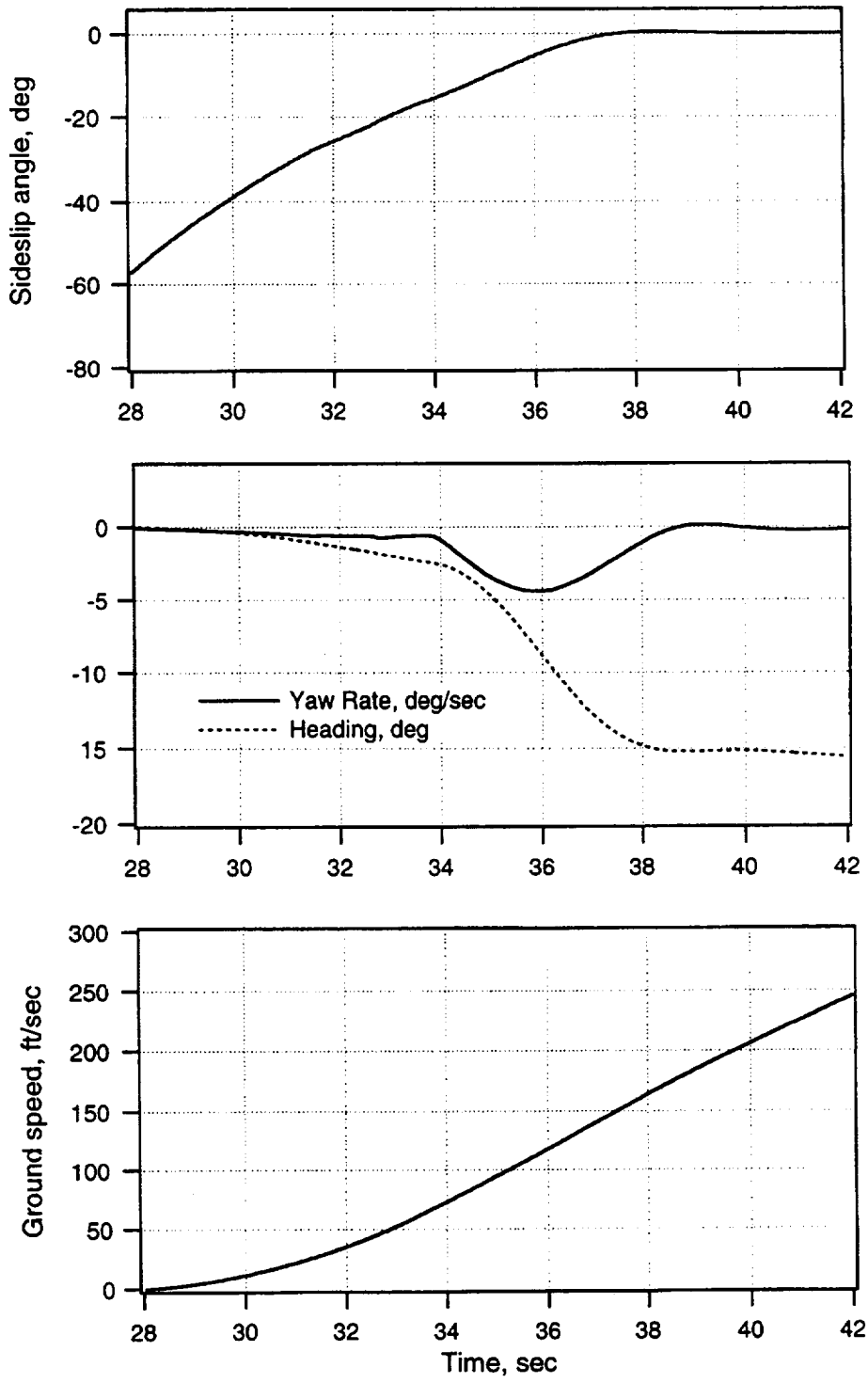

Figure 28(b). Yaw response during acceleration from hover in 15 knot crosswind for yaw mode blending range from 40 to 100 knots.

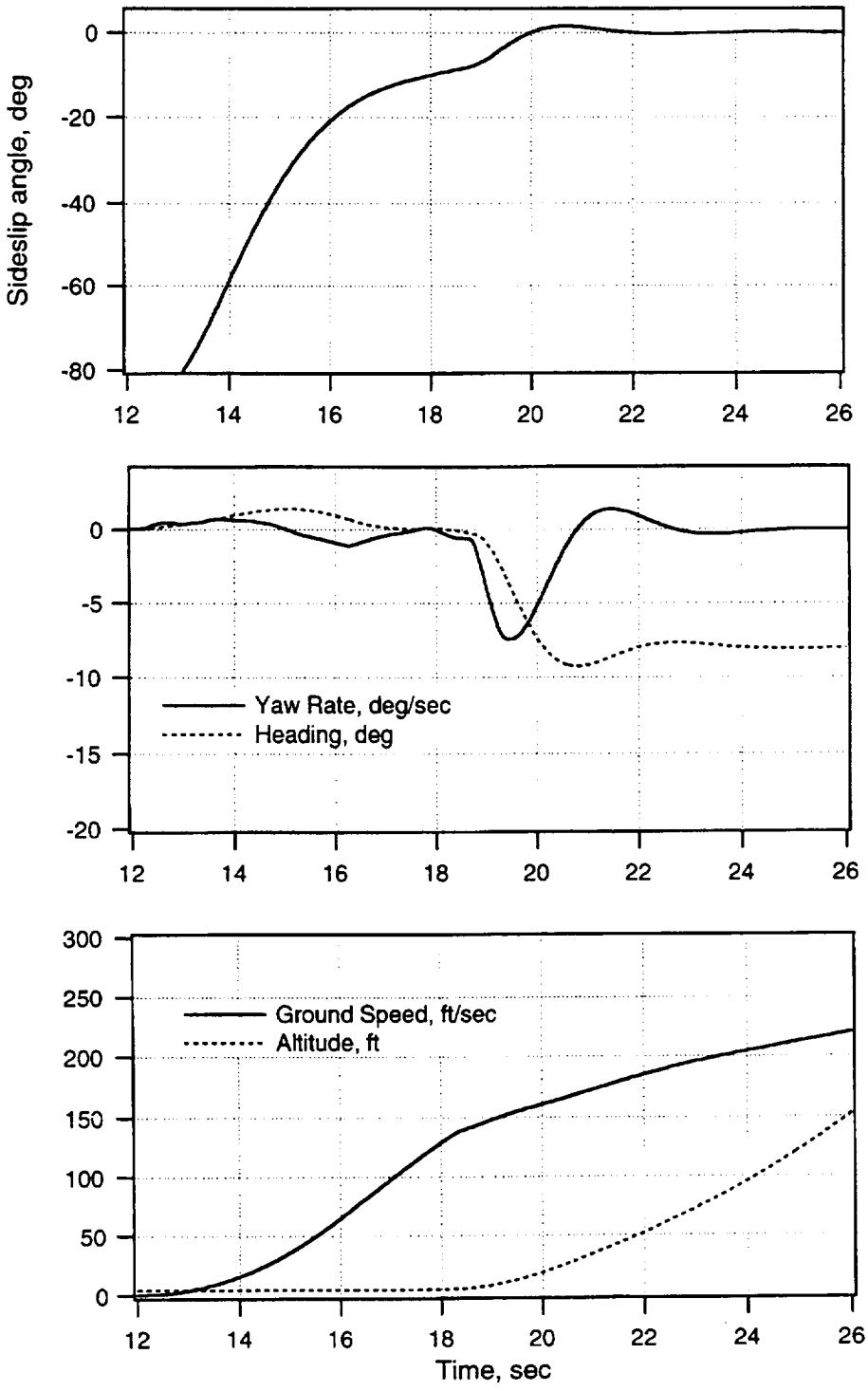

Figure 29(a). Yaw response during short takeoff in 15 knot crosswind for yaw mode blending range from 40 to 60 knots.

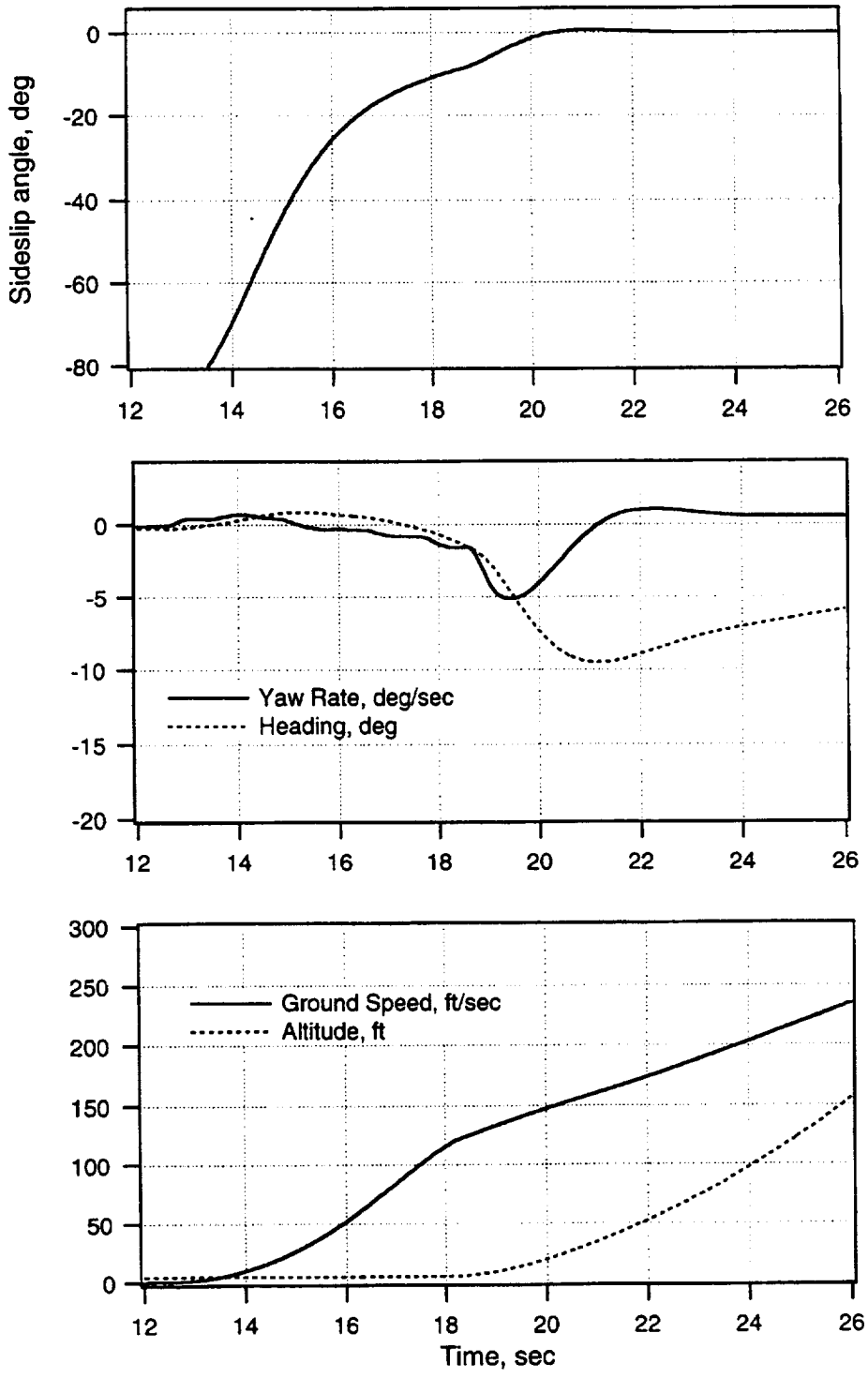

Figure 29(b). Yaw response during short takeoff in 15 knot crosswind for yaw mode blending range from 40 to 100 knots.

REPORT DOCUMENTATION PAGE

Form Approved
OMB No. 0704-0188

1. AGENCY USE ONLY *(Leave blank)*	2. REPORT DATE	3. REPORT TYPE AND DATES COVERED
	November 1997	Technical Memorandum

4. TITLE AND SUBTITLE

Moving-Base Simulation Evaluation of Control/Display Integration Issues for ASTOVL Aircraft

5. FUNDING NUMBERS

581-50-22

6. AUTHOR(S)

James A. Franklin

7. PERFORMING ORGANIZATION NAME(S) AND ADDRESS(ES)

Ames Research Center
Moffett Field, CA 94035-1000

8. PERFORMING ORGANIZATION REPORT NUMBER

A-977540

9. SPONSORING/MONITORING AGENCY NAME(S) AND ADDRESS(ES)

National Aeronautics and Space Administration
Washington, DC 20546-0001

10. SPONSORING/MONITORING AGENCY REPORT NUMBER

NASA TM-112213

11. SUPPLEMENTARY NOTES

Point of Contact: James A. Franklin, Ames Research Center, MS 211-2, Moffett Field, CA 94035-1000
(650) 604-6004

12a. DISTRIBUTION/AVAILABILITY STATEMENT

Unclassified — Unlimited
Subject Category 08

12b. DISTRIBUTION CODE

13. ABSTRACT ***(Maximum 200 words)***

A moving-base simulation has been conducted on the Vertical Motion Simulator at Ames Research Center using a model of an advanced, short takeoff and vertical landing (STOVL) lift fan fighter aircraft. This experiment expanded on investigations during previous simulations with this STOVL configuration with the objective of evaluating (1) control law modifications over the low speed flight envelope, (2) integration of the throttle inceptor with flight control laws that provide direct thrust command for conventional flight, vertical and short takeoff, and flightpath or vertical velocity command for transition, hover, and vertical landing, (3) control mode blending for pitch, roll, yaw, and flightpath control during transition from wing-borne to jet-borne flight, and (4) effects of conformal versus nonconformal presentation of flightpath and pursuit guidance symbology on the out-the-window display for low speed STOVL operations. Assessments were made for takeoff, transition, hover, and landing, including precision hover and landing aboard an LPH-type amphibious assault ship in the presence of winds and rough seas.

Results yielded Level 1 pilot ratings for the flightpath and vertical velocity command modes for a range of land-based and shipboard operation and were consistent with previous experience with earlier control laws and displays for this STOVL concept. Control mode blending was performed over speed ranges in accord with the pilot's tasks and with the change of the basic aircraft's characteristics between wing-borne and hover flight. Blending of yaw control from heading command in hover to sideslip command in wing-borne flight performed over a broad speed range helped reduce yaw transients during acceleration through the low speed regime. Although the pilots appreciated conformality of flightpath and guidance symbols with the external scene during the approach, increased sensitivity of the symbols for lateral path tracking elevated the pilots' control activity in the presence of turbulence. The pilots preferred the choice of scaling that was originally established during the display development and in-flight evaluations.

14. SUBJECT TERMS	15. NUMBER OF PAGES
STOVL, V/STOL, Flight/propulsion system, Flying qualities, Simulation	59
	16. PRICE CODE: A04

17. SECURITY CLASSIFICATION OF REPORT	18. SECURITY CLASSIFICATION OF THIS PAGE	19. SECURITY CLASSIFICATION OF ABSTRACT	20. LIMITATION OF ABSTRACT
Unclassified	Unclassified		